



HAL
open science

Predicting the structure and functions of peatland microbial communities from Sphagnum phylogeny, anatomical and morphological traits and metabolites

Anna Sytiuk, Régis Céréghino, Samuel Hamard, Frédéric Delarue, Amélie Guittet, Janna Barel, Ellen Dorrepaal, Martin Küttim, Mariusz Lamentowicz, Bertrand Pourrut, et al.

► To cite this version:

Anna Sytiuk, Régis Céréghino, Samuel Hamard, Frédéric Delarue, Amélie Guittet, et al.. Predicting the structure and functions of peatland microbial communities from Sphagnum phylogeny, anatomical and morphological traits and metabolites. *Journal of Ecology*, 2021, 10.1111/1365-2745.13728 . hal-03373855

HAL Id: hal-03373855

<https://hal.science/hal-03373855>

Submitted on 15 Nov 2021

HAL is a multi-disciplinary open access archive for the deposit and dissemination of scientific research documents, whether they are published or not. The documents may come from teaching and research institutions in France or abroad, or from public or private research centers.

L'archive ouverte pluridisciplinaire **HAL**, est destinée au dépôt et à la diffusion de documents scientifiques de niveau recherche, publiés ou non, émanant des établissements d'enseignement et de recherche français ou étrangers, des laboratoires publics ou privés.

1

2 **Predicting the structure and functions of peatland microbial communities**
3 **from *Sphagnum* phylogeny, anatomical and morphological traits and**
4 **metabolites**

5 Anna Sytiuk^{1*}, Regis Céréghino¹, Samuel Hamard¹, Frédéric Delarue², Amélie Guittet², Janna M.
6 Barel¹, Ellen Dorrepaal³, Martin Küttim⁴, Mariusz Lamentowicz⁵, Bertrand Pourrut¹, Bjorn J.M.
7 Robroek^{6,7}, Eeva-Stiina Tuittila⁸, Vincent E.J. Jassey¹

8 ¹Laboratoire Ecologie Fonctionnelle et Environnement, Université de Toulouse, UPS, CNRS, Toulouse,
9 France,

10 ²Sorbonne Université, CNRS, EPHE, PSL, UMR 7619 METIS, 4 place Jussieu, F-75005 Paris, France

11 ³Climate Impacts Research Centre, Department of Ecology and Environmental Science, Umeå University,
12 SE-981 07, Abisko, Sweden,

13 ⁴Institute of Ecology, School of Natural Sciences and Health, Tallinn University, Uus-Sadama 5, 10120
14 Tallinn, Estonia,

15 ⁵Climate Change Ecology Research Unit, Faculty of Geographical and Geological Sciences, Adam
16 Mickiewicz University in Poznań, Bogumiła Krygowskiego 10, 61-680 Poznań, Poland,

17 ⁶Aquatic Ecology & Environmental Biology, Institute for Water and Wetland Research, Faculty of Science,
18 Radboud University Nijmegen, AJ 6525 Nijmegen, The Netherlands,

19 ⁷Biological Sciences, Faculty of Natural and Environmental Sciences, Institute for Life Sciences, University
20 of Southampton, Southampton SO17 1BJ, UK

21 ⁸School of Forest Sciences, Joensuu campus, University of Eastern Finland, Finland.

22

23 *corresponding author: anna.sytiuk@univ-tlse3.fr

24 Abstract

- 25 1. *Sphagnum* mosses are keystone species in northern peatlands. Notably, they play an important
26 role in peatland carbon (C) cycling by regulating the composition and activity of microbial
27 communities. However, it remains unclear whether information on *Sphagnum* phylogeny and/or
28 traits-based composition (*i.e.* anatomical and morphological traits and metabolites) can be used
29 to predict the structure of microbial communities and their functioning. Here we evaluated
30 whether *Sphagnum* phylogeny and traits predict additional variation in peatland microbial
31 community composition and functioning beyond what would be predicted from environmental
32 characteristics (*i.e.* climatic and edaphic conditions).
- 33 2. We collected *Sphagnum* and microbial data from five European peatlands distributed along a
34 latitudinal gradient from northern Sweden to southern France. This allowed us to assess
35 *Sphagnum* anatomical and morphological traits and metabolites at different sites along changing
36 environmental conditions. Using structural equation modelling (SEM) and phylogenetic distance
37 analyses, we investigated the role of *Sphagnum* traits in shaping microbial community
38 composition and functioning along with environmental conditions.
- 39 3. We show that microbial community composition and traits varied independently from both
40 *Sphagnum* phylogeny and the latitudinal gradient. Specifically, the addition of *Sphagnum* traits to
41 climatic and edaphic variables to the SEM allowed it to explain a larger proportion of the explained
42 variance (R^2). This observation was most apparent for the biomass of decomposers (+42%) and
43 phototrophs (+19%), as well as for growth yield microbial traits (+10%). As such, that *Sphagnum*
44 metabolites were important drivers for microbial community structure and traits, while
45 *Sphagnum* anatomical and morphological traits were poor predictors.

46 4. *Synthesis*. Our results highlight that *Sphagnum* metabolites are more to influence peatland
47 microbial food web structure and functioning than *Sphagnum* anatomical and morphological
48 traits. We provide further evidence that measurements of the plant metabolome, when combined
49 with classical functional traits, improve our understanding of how the plants interact with their
50 associated microbiomes.

51

52 **Key-words:** Functional traits, Latitudinal gradient, Metabolomics, Microbial traits, Peatlands, Plant and
53 microbial communities, Plant–soil (below- ground) interactions, *Sphagnum*

54

55

56 **Introduction**

57 Soil microbial communities are highly diverse and make a significant contribution to many critical
58 ecosystem functions (Crowther et al., 2019), such as the decomposition of plant litter (Geisen, 2020;
59 Schlesinger & Andrews, 2000; Singh et al., 2010), nutrient cycling (Gui et al., 2017), and the mineralization
60 and stabilization of soil organic matter (Liang et al., 2017, 2019). Moreover, soil microorganisms are
61 interconnected with plants. By aiding plant nutrient acquisition (Averill et al., 2019) and drought
62 resistance (Mariotte et al., 2015), soil microorganisms play a key role in shaping plant productivity and
63 community dynamics (Mommer et al., 2018; Wardle et al., 2004). Plants, in turn, determine the
64 composition of soil communities by regulating surface soil temperature and hydrology, as well as the
65 chemical signature of organic carbon inputs (litter) and rhizodeposits (Bardgett & Wardle, 2010).

66 Biotic and abiotic factors influence the composition of soil microbial communities. Climatic (*e.g.*
67 temperature, precipitation) and edaphic conditions (*e.g.* soil pH, moisture) are often seen as important
68 determinants of microbial communities (Borowik & Wyszowska, 2016; Singh et al., 2009; Wang et al.,
69 2020) yet they cannot completely explain the full variation observed within microbial communities (De
70 Gruyter et al., 2020). This suggests that biotic interactions also play an important role in shaping microbial
71 communities (Geisen, 2020). Trophic and non-trophic (*e.g.* competition) interactions among
72 microorganisms are important, but often neglected (Gralka et al., 2020). Recently, plant species identity
73 (Burns et al., 2015), plant phylogeny (Barberán et al., 2015) and plant community composition (de Vries
74 et al., 2012; Robroek et al., 2015) have also been identified as important drivers of microbial communities.
75 However, disparity remains once individual plant leaf and root traits are taken into account (Leff et al.,
76 2018), suggesting that plant traits are poor predictors of microbial communities and microbial processes
77 (see Sweeney et al., 2020). Alternatively, the effect of plant species identity and/or community
78 composition on microbial communities may mostly rely on chemical interactions between plant and soil

79 microbes (van Dam & Bouwmeester, 2016). Plants produce a plethora of biochemicals, and can release
80 over a hundred different metabolites in their surroundings that can attract, deter, or even kill
81 belowground microbes (Fernandez et al., 2016; Hamard et al., 2019; Hu et al., 2018; Pinton et al., 2001).
82 Elucidating which plant characteristics (phylogeny, morphological and anatomical traits and/or
83 metabolites) govern microbial communities, particularly in addition to microbial interactions and climatic
84 and edaphic conditions, is thus urgently needed to predict the structure of microbial communities, their
85 functioning and subsequent ramifications for biogeochemical cycles (Bardgett & Wardle, 2010).

86 We address this knowledge gap by examining the understudied linkages between peat mosses
87 (*i.e.* *Sphagnum* moss) and their associated microbiome. *Sphagnum*-dominated peatlands store more
88 carbon (C) than any other terrestrial ecosystem (Nichols & Peteet, 2019). Carbon accumulation in
89 *Sphagnum*-peatlands results from cold, acidic, nutrient-poor and water-saturated conditions that have
90 hindered microbial decomposition of litter over millennia (Rydin & Jeglum, 2006). *Sphagnum* mosses also
91 facilitate their own growth by creating unfavorable conditions for vascular plants, generating recalcitrant
92 litter and changing physical and chemical properties of the soil (Turetsky, 2003; van Breemen, 1995). As
93 *Sphagnum* do not possess roots, the leaf-associated microbiome comprises crucial functions, such as
94 defenses against pathogen and additional nutrient supply for *Sphagnum* growth and development (Opelt,
95 et al., 2007b). The association between *Sphagnum* moss and its microbiome, *i.e.* the bryosphere (*sensu*
96 Lindo & Gonzalez, (2010)), plays a key role in peatland C dynamics. These *Sphagnum*-associated microbial
97 communities include a core detrital network for C and nutrient cycling (Gilbert et al., 1998; Jassey et al.,
98 2015; Lindo & Gonzalez, 2010). Unique anatomical and morphological traits of *Sphagnum*, especially the
99 cell structure of leaves - with one layer of photosynthetically active cells (chlorocystes) and dead, water-
100 filled hyaline cells, create consistent microenvironments for the microbial communities (Bragina et al.,
101 2012a). Large hyaline cells can serve as less acidic 'oases' for microorganisms in the otherwise acidic
102 peatland pore water (Kostka et al., 2016). *Sphagnum* also actively excretes bioactive metabolites (*i.e.*

103 biochemicals) to their surroundings such as polyphenols (Rasmussen et al., 1995a; Rasmussen et al.,
104 1995b; Rudolph & Samland, 1985; Schellekens et al., 2015), flavonoids (Sytiuk et al., 2020), carbohydrates
105 (Hájek et al., 2011; Painter, 1991; Tetemadze et al., 2018; van Breemen, 1995), and tannins (Sytiuk et al.,
106 2020; Verhoeven & Liefveld, 1997), that have been related to the functioning of peatlands (Verhoeven &
107 Liefveld, 1997). Many of these metabolites show antimicrobial properties (Fudyma et al., 2019). For
108 example, *Sphagnum* phenolics have been suggested to reduce vascular plant's mycorrhization (Binet et
109 al. 2017; Chiapusio et al., 2018), and inhibit bacterial growth (Mellegård et al., 2009), decomposition
110 (Freeman et al., 2001; Verhoeven & Liefveld, 1997; Verhoeven & Toth, 1995) and microbial respiration
111 (Hamard et al., 2019). As *Sphagnum* species engineer their environment (van Breemen, 1995; Bengtsson
112 et al., 2016; Bengtsson et al., 2018), both *Sphagnum* anatomical/morphological and biochemical traits
113 may be expected to steer the structure and function of peatland microbial communities. A better
114 identification and comprehension of these drivers are crucial for predicting the composition of the
115 microbial community and its functioning in peatlands.

116 Here, we explore how and to what extent *Sphagnum* phylogeny, anatomical and morphological
117 traits and metabolites drive the spatial variability of microbial community composition and functioning.
118 To do so, we conducted an observational study in five European *Sphagnum*-dominated peatlands
119 representing a wide range of climatic and edaphic conditions. Because *Sphagnum* microbial community
120 composition can vary across space (Mitchell et al., 2003; Robroek et al., 2021), and according to the
121 variation of edaphic factors such as pH and nutrient richness (Bragina et al., 2013a; Jassey et al., 2014;
122 Opelt et al., 2007a), we hypothesized that (1) microbial community composition and functional traits will
123 show distinct patterns among the five peatlands. We expected (2) that geographical variation in microbial
124 community composition and microbial traits is driven by climatic/edaphic conditions as well as *Sphagnum*
125 anatomical and morphological traits and metabolites. In particular, we hypothesized that (3) *Sphagnum*
126 traits will explain a fraction of variation in microbial community composition and microbial traits that is

127 not explained by climatic and edaphic conditions. Among *Sphagnum* traits, we predicted that (4)
128 *Sphagnum* metabolites have a stronger effect in shaping microbial properties than anatomical and
129 morphological traits, since metabolites are released into *Sphagnum* surroundings and can directly
130 influence microbial community composition and/or microbial traits. Finally, as *Sphagnum* traits do not
131 exclusively vary with climatic and edaphic conditions (Sytiuk et al., 2020), but also according to phylogeny
132 (Laine et al., 2021), we hypothesized that (5) *Sphagnum* phylogeny is an important determinants of
133 microbial properties, in addition to climatic and edaphic conditions and *Sphagnum* traits.

134 **Material and methods**

135 **Sites, sampling design and sample collection**

136 We selected five *Sphagnum*-dominated peatlands along a latitudinal gradient from northern Sweden to
137 southern France to represent a wide range of edaphic and climate conditions (Table 1, Table S1, S3). In
138 each site, a preliminary vegetation survey (see Table S2) allowed us to select five homogeneous plots (50
139 x 30 cm each; 5 plots x 5 sites = 25 plots in total) dominated by a single *Sphagnum* species: *S. warnstorffii*
140 (France, FR), *S. magellanicum* (Poland, PL), *S. rubellum* (Estonia, EST), *S. papillosum* (Finland, FI) and *S.*
141 *balticum* (Sweden, SE). Dominant *Sphagnum* species were site specific, potentially creating a confounding
142 effect with climate/edaphic conditions. To overcome this issue, we measured phylogenetic differences
143 among *Sphagnum* species at five sites, and found that *Sphagnum* phylogeny did not covary with climatic
144 variation (*i.e.* mean annual temperature, $F_{1,3} = 0.15$, $P = 0.72$, Fig. S1). Despite the absence of phylogeny-
145 climate covariation, it remains true that species identity and site variation were still potentially
146 confounding. We thus quantified metabolite plasticity (*i.e.*, water-soluble phenols) of the five *Sphagnum*
147 species using a reciprocal transplantation along the latitudinal gradient to determine whether *Sphagnum*
148 metabolite production is more sensitive to environmental variability than to taxonomy. We found that
149 the concentration of water-soluble phenols increased for all *Sphagnum* species along the latitudinal
150 gradient (Fig S2a, b), and more importantly that the variance of water-soluble phenol concentrations
151 within the same species at different temperatures was higher than between the different species at the
152 same temperature (Fig. S2c). Together, these findings show that water-soluble phenol concentrations in
153 *Sphagnum* tissues vary independently of taxonomy. However, other metabolites may depend on
154 taxonomy. To exclude this potential, we used unpublished data (Jassey, Allard and Robroek, unpublished
155 data) on *Sphagnum* metabolomic profiling from 56 European ombrotrophic peatlands (see sites in
156 Robroek et al., 2017). A PCoA analysis revealed that that the metabolomic composition of *Sphagnum*

157 species was strongly determined by local and regional conditions (site effect, $P < 0.05$), rather than by
158 taxonomy (species effect, $P = 0.46$; Fig. S3). Altogether, these additional analyses demonstrate that a
159 potential confounding effect of species and site was not an important issue when referring to *Sphagnum*
160 metabolites. However, we acknowledge that anatomical and morphological traits are used to identify
161 *Sphagnum* moss to species (Isoviita, 1966), and that in our study anatomical and morphological traits
162 cannot be disentangled from *Sphagnum* taxonomy. We therefore advise caution when using these data
163 to predict microbial communities and microbial activities.

164 In each plot, 15-20 *Sphagnum* shoots were sampled around ten marked spots (ca. 250 g fresh
165 weight of *Sphagnum* per plot). This sampling design allowed us to obtain a composite sample,
166 representative of the entire plot. Upon sampling, the living top of the *Sphagnum* shoots (0-3 cm) were cut
167 immediately, pooled, homogenized and then dispatched for the different lab analyses. Approximately 10
168 g of *Sphagnum* shoots were fixed in 20 mL of glutaraldehyde (2% final concentration) and stored at 4°C in
169 the dark for microbial biomass/abundance measurements. Approximately 20 g were frozen and
170 lyophilized for fungal and biochemical analyses. Another 10 g were frozen for analyses of microbial
171 enzymatic activities. The remaining 10 g were stored at 4°C and used for analyses of *Sphagnum* anatomical
172 and morphological traits. We collected *Sphagnum* samples in every site within the same week in early-
173 July 2018.

174 **Characterizing climate and site conditions**

175 For each site, we extracted bioclimatic data from WorldClim v2 (Fick & Hijmans, 2017): mean annual
176 temperature, temperature seasonality, annual precipitation, and precipitation seasonality averaged over
177 the 1960-2018 period (Table S1). Water-table depth (WTD) and pH were measured directly in the field
178 using a ruler and a portable multimeter Elmetron CX742, respectively (Table 1). Water-extractable organic
179 matter (WEOM) was extracted from the *Sphagnum* shoots (0-3 cm height) collected at the five sites

180 according to Jassey et al. (2018) (Table S3). Briefly, *Sphagnum* shoots were soaked in 30 mL of
181 demineralized water and then shaken for 90 min at 150 rpm. *Sphagnum* shoots were then dried at 60°C
182 for 48 hours and weighted to obtain dry mass (mg/g DW). The water extract was filtered with Whatman
183 filter (1 µm pore size) and several physical-chemical parameters were analyzed: a TOC analyser (Shimadzu
184 TOC-L) was used to quantify dissolved organic carbon, nitrogen and phosphate (WEOC, WEON and WEOP
185 respectively). To measure dissolved organic matter aromatic content and molecular weight (WEOCq), we
186 used absorbance measurements between 250 and 660 nm (15 wavelengths in total) in 200 µL sample
187 aliquots in 96-well quartz microplate using a BioTek SynergyMX spectrofluorometer (Jaffrain et al., 2007).
188 For a blank, we used demineralized water filtered through Whatman filter to correct our values for the
189 potential C released from the filter. Spectral slopes ($S_{250-660}$, nm⁻¹) were calculated using linear least
190 squares regressions with Ln-transformed absorptions. High $S_{250-660}$ values indicate low molecular weight
191 material (Hansen et al., 2016).

192 We further performed a vegetation survey using two high-resolution images (25 x 15 cm) of each
193 plot, according to Buttler et al. (2015). On each picture, we laid a grid of 336 points and identified species
194 overlaying the grid intersects. This technique did not assess vertical biomass and could underestimate the
195 relative abundance of certain species. However, the bias was alike in each plot, making species
196 frequencies comparable among sites.

197 ***Sphagnum* anatomical and morphological traits**

198 We characterized a suite of four anatomical and morphological *Sphagnum* traits determining the capacity
199 of *Sphagnum* moss to provide shelter for microbial communities following Jassey & Signarbieux (2019):
200 volume of the capitulum (height x diameter of capitulum), water-holding capacity of the capitulum and
201 shoot, number of hyaline cells per leaf area (*i.e.* dead cells storing water), the surface area of hyaline cell
202 (length x width) and width of chlorocystes (photosynthetic cells surrounding hyaline cells). In total, 125

203 individuals (25 per site) were randomly collected to estimate the volume of the capitula (mm^3) by
204 measuring their height and diameter using a precision ruler. Then, we used the same samples to quantify
205 the net water content of the capitula and stem (first cm) at water saturation. Capitula and stems were
206 submerged in water until their maximum water retention capacity was reached. Excess water was
207 removed by allowing water to drain naturally for two minutes. Then, individual capitula and stems were
208 weighed as water-saturated and subsequently dried for three days at 60°C . The net water content at
209 water saturation of each individual was expressed in grams of water per gram of dry mass ($\text{g H}_2\text{O/g DW}$).
210 For anatomical analyses, we carefully deconstructed five *Sphagnum* capitula in each plot (in total, 125
211 capitula) to isolate *Sphagnum* leaves. Then, we pooled all *Sphagnum* leaves, homogenized, and took three
212 leaves from that pool to prepare microscope slides from each plot (375 leaves analyzed in total). We
213 quantified the number of hyaline cells per leaf area (number of hyaline cells per mm^2), their surface (μm^2),
214 as well as the width of chlorocystes (μm), using a light microscope connected to a camera (LEICA ICC50
215 HD) and the size analytic tools (LEICA suite software).

216 ***Sphagnum* metabolic fingerprint**

217 We assessed the metabolic fingerprint of *Sphagnum* mosses using two different approaches. First, we
218 quantified a set of nine moss metabolites that can influence microbes. The different extractions pathways
219 used for quantifying the various *Sphagnum* metabolites are detailed in Sytiuk et al. (2020). Briefly,
220 *Sphagnum* mosses were frozen, lyophilized, ground and stored at -20°C prior to biochemical analysis.
221 Then, we used (i) a 99.9% methanol extraction for quantifying *Sphagnum* pigments (chlorophyll a, b and
222 total carotenoids), (ii) a 50% methanol extraction for quantifying total polyphenols, flavonoids, tannins
223 and carbohydrates, (iii) a water extraction for quantifying water-extractable total polyphenols, (iv) a
224 sulfosalicylic acid extraction for quantifying proline and (v) a dosage of proteins with bovine serum
225 albumin (BSA). All metabolites were quantified using spectroscopy at different wavelengths. Secondly, we

226 characterized the polysaccharides, aromatic and aliphatics content of *Sphagnum* mosses using Fourier
227 Transform Infrared Spectroscopy (FT-IR-ATR; (Hodgkins et al., 2014). 30 mg freeze-dried and ground
228 *Sphagnum* was placed directly on a germanium crystal and pressed down with a flat tip to improve
229 distribution and contact. Spectra were acquired by 64 scans at a 2 cm^{-1} resolution over the range 4000–
230 600 cm^{-1} . All spectra were corrected for water vapor, CO_2 and for differences in depth of beam penetration
231 at different wavelengths (ATR correction; Opus software). All spectra were then normalized. For each
232 spectrum, normalization involved (i) a subtraction of the minimum absorption value applied to the whole
233 spectrum followed by (ii) a multiplication - also applied on the whole spectra - to obtain a spectral maximal
234 absorbance value of 1 for each *Sphagnum* sample. Six main absorption peaks were used as an indicator
235 of *Sphagnum* polysaccharides, aromatics and aliphatics: 1) the 1064 cm^{-1} region (combination of C–O
236 stretching and O-H deformation) is associated to polysaccharides; 2) the 1515 cm^{-1} region (C=C; aromatic
237 compounds) is assigned to lignin/phenolic backbone; 3) the 1610 cm^{-1} region (C=C stretching; aromatic
238 compounds and/or asymmetric C-O stretch in COO^-) is associated to lignin and other aromatics, or
239 aromatic or aliphatic carboxylates; 4) the 1724 cm^{-1} - 1710 cm^{-1} region (C=O stretch of COOH or COOR)
240 corresponds to free organic acids, carboxylic acids, aromatic esters; 5) 2850 cm^{-1} region (symmetric CH_2)
241 is associated to aliphatics; and 6) 2920 cm^{-1} region (antisymmetric CH_2) is associated to aliphatics. We used
242 the ratio between the relative intensities of FT-IR absorption bands, where 1610 cm^{-1} region was used as
243 denominator due to its highly recalcitrant nature, in order to evaluate *Sphagnum* fingerprints and their
244 degree of degradability.

245 **Microbial abundances and biomass**

246 Microbial consumers (testate amoebae, ciliates, rotifers and nematodes), phototrophs (microalgae and
247 cyanobacteria), and decomposers (fungi and bacteria) were extracted from *Sphagnum* following Jassey et
248 al. (2011a). For bacterial counts, a 1-mL sub-sample was stained with SYBR Green (0.1x final

249 concentration) and incubated in the dark for 15 minutes. Then the sub-samples were run at a speed of 2
250 $\mu\text{L s}^{-1}$ at a count rate not exceeding 1000 events s^{-1} in a cytometer (Guava® easyCyte). Epifluorescence
251 microscopy was used to determine the size of bacteria: 1 mL sub-samples were stained with DAPI (4,6-
252 diamino-2-phenylindole; 3 $\mu\text{g mL}^{-1}$ final concentration), incubated in the dark for 15 minutes, filtered on
253 0.2 μm black membrane filters and examined by fluorescence microscopy at 1000x magnification.
254 Bacterial sizes were determined manually under the microscope following Jassey et al. (2011a). The
255 abundance of phototrophs and microbial consumers, as well as their identification to species level when
256 possible, was carried out using a 3-mL subsample and inverted microscopy ($\times 400$, Utermöhl method). The
257 abundance of bacteria, phototrophic and consumer species was then converted into biovolume (μm^3),
258 calculated based on geometrical shapes using dimensions measured under the microscope (length or
259 diameter; width, and height). Biovolumes were converted to biomass (μgC) using conversion factors as
260 given in Gilbert et al. (1998). The biomass data were expressed in micrograms of C per gram of *Sphagnum*
261 dry mass ($\mu\text{g C g}^{-1}$ DM). The biomass of fungi was quantified using ergosterol quantification according to
262 the standard extraction procedure previously described in Gessner et al. (1991). Briefly, 50 mg of
263 lyophilized *Sphagnum* were incubated in glass vials with 5 mL of potassium hydroxide methanol (8 g L^{-1})
264 for 24h at 4°C. A control vial containing 100 μL of a 200- $\mu\text{g mL}^{-1}$ solution of ergosterol was also incubated
265 in the same conditions to take into account the yield of the extraction. All vials were then heated at 80°C
266 for 30 min. After cooling, 1 mL of hydrochloric acid (0.65 mol L^{-1}) was added in each sample. 3mL of each
267 sample were filtered on Oasis HLB cartridges (60 mg sorbent, 30 μm particle size). Cartridges were
268 previously and successively conditioned with 1 mL of methanol and 1 mL of a mixture of 15%v methanol,
269 70%v potassium hydroxide methanol (8 g L^{-1}) and 15%v hydrochloric acid (0.65 mol L^{-1}). After sample
270 filtration, cartridges were washed with 1 mL of 5%v methanol diluted in autoclaved milli-Q water.
271 Cartridges were then dried under vacuum (-5 bar) for 1 h, after what they were eluted with 4*350 μL of
272 isopropanol. The concentration of ergosterol in eluates was assessed by HPLC, using a calibration curve.

273 The yield of the extraction was assessed by comparing the measured and theoretical concentration of
274 ergosterol in the control vial. Ergosterol concentrations in samples were corrected from the yield of the
275 reaction and were expressed in μg of ergosterol per g of *Sphagnum* dry weight.

276 **Microbial traits**

277 Following the revised life history theory for microbial traits (Malik et al., 2020), we collected microbial
278 traits classified into three main microbial life history strategies: growth yield, resource acquisition and
279 stress tolerance. We quantified nine traits in the growth yield strategy: biomass per cell, biovolume per
280 cell, body size (length and width), the quantum yield of photosystem II for phototrophs, photosynthetic
281 pigments content per cell for phototrophs, growth rate, reproduction rate, and respiration rate per cell.
282 We classified 14 traits in the resource acquisition strategy: nine microbial enzyme activities, C uptake by
283 phototrophs, predation rates, nitrogen fixation, methanotrophy and motility. Finally, three traits were
284 assigned to the stress tolerance strategy: morphology, response to temperature increase, and tolerance
285 to desiccation. A total of 26 microbial traits were either directly quantified or acquired from the literature
286 (see Supplementary method on microbial traits for more details).

287 To describe the functional trait space in each site, we calculated community weighted means
288 (CWM) of each trait calculated as the presence/absence weighted means of species trait values using the
289 FD R package (Laliberté et al., 2015). We then created a functional distance matrix by applying Gower's
290 distance on each pair of species described by their traits, and then computed a Principal Coordinate
291 Analysis (PCoA) on it. Gower's distance allows mixing of different types of traits (*i.e.* qualitative and
292 quantitative traits) while giving them equal weights. Then, the two first axes of the PCoA were selected as
293 synthetic CWMs summarizing the microbial functional space in each site.

294 Numerical analyses

295 All statistical analyses were performed in R 3.5.3 (R Core Team, 2019) using packages, as specified below.
296 Linear mixed effects models were used to assess the *Sphagnum* taxonomy effect (fixed effect) on the
297 microbial biomass of each trophic group, CWM of each microbial trait and *Sphagnum* traits. The models
298 were fitted with plot nested within *Sphagnum* taxonomy as a random effect on the intercept (Pineiro &
299 Bates, 2000). Tukey's multiple comparison test was used for *post hoc* analyses of differences among the
300 levels of the fixed effects in the final model. Normality and homogeneity assumptions of the data, as well
301 as model residuals, were assessed using a Shapiro test and diagnostic plots. Log₁₀-transformations of the
302 data were applied if needed in order to meet these assumptions. To represent differences in microbial
303 community composition, microbial trait composition and *Sphagnum* traits, we performed principal
304 coordinate analysis (PCoA) using Gower's distance that allowed mixing of different types of data (*i.e.*
305 qualitative and quantitative traits) while giving them equal weights. A standardization (*Sphagnum*
306 anatomical and morphological traits and metabolites) or Hellinger transformation (microbial community
307 composition and microbial traits) was applied on the matrices beforehand (Legendre & Legendre, 2012).
308 We used Spearman correlations to test the potential relationships between microbial community
309 composition, CWM of microbial traits and *Sphagnum* traits and/or climatic and edaphic factors.

310 We assessed the effect of *Sphagnum* phylogenetic distance on microbial biomass and microbial
311 trait composition under the Brownian Motion model (BM). BM predicts that the variance in microbial
312 properties increases at a constant rate proportionate to the evolutionary distance among *Sphagnum*
313 species, with more closely related species having more similar values for microbial properties, and
314 indicating that the variable has a phylogenetic signal (Felsenstein, 1985). We used Blomberg's K index
315 (Münkemüller et al., 2012) to test for a *Sphagnum* phylogenetic signal among microbial variables with
316 randomization and 1000 permutations (Table S4).

317 To assess whether differences in *Sphagnum* anatomical and morphological traits and metabolites
318 predicted variation in microbial community composition and microbial traits beyond the explanatory
319 power of climatic and edaphic conditions (Leff et al., 2018), we built a set of path diagrams subjected to
320 structural equation modelling (Grace et al., 2010, 2014). We compared the explanatory power of the
321 models, assessed through adjusted R^2 values and Akaike Information Criterion (AIC), by framing four types
322 of models (Fig. 1). First, we tested the effects of climatic and edaphic conditions on each (hereafter ‘single’
323 SEM models) trophic group (*i.e.* the biomass of either decomposers, phototrophs, predators or the total
324 microbial biomass) and microbial trait strategy (*i.e.* either growth yield, resource acquisition and stress
325 tolerance strategies or the overall traits composition; Fig. 1a) separately. Second, we tested the effects of
326 climatic and edaphic conditions on the interactions (hereafter ‘interactions’ SEM model) among/within
327 microbial community composition and microbial trait strategies (Fig. 1b). Third, we tested the effect of
328 *Sphagnum* anatomical and morphological traits and metabolites (*i.e.* *Sphagnum* traits; in addition to
329 climatic and edaphic conditions as in the first model) on each trophic group and microbial trait strategy
330 separately (Fig. 1c) and in interaction (Fig. 1d). The benefits gained (ΔR^2) by including *Sphagnum*
331 anatomical and morphological traits and metabolites into the models were calculated as follows:

$$332 \quad \Delta R^2 = (R^2_{SEM \text{ with } Sphagnum \text{ traits}} - R^2_{SEM \text{ without } Sphagnum \text{ traits}}) * 100\%$$

333 We further compared AIC values between models with and without *Sphagnum* traits to check for potential
334 overfitting (Burnham & Anderson, 2004). In these models, we used annual precipitation and mean
335 temperature of the wettest quarter as climate variables, selected beforehand using a principal component
336 analysis (PCA) applied on all bioclimatic variables. For edaphic peatland conditions, we used *Sphagnum*
337 water content and the first axis of a PCA applied on WEON, WEOC, WEOP and $S_{260-660}$. For microbial trait
338 strategies, we used the first axis of three PCoAs applied on the CWM of traits of each trait strategy,
339 respectively. The paths of the SEM were fitted as previously described for ANOVAs using *piecewiseSEM*

340 package (Lefcheck, 2016). We selected this approach as it allowed using the Shipley's test of d-separation
341 to assess whether direct or indirect paths are missing from the *a priori* model. The adequacy of the model
342 was evaluated via several tests including non-significant *Fisher's C* statistic ($P > 0.05$), and low Akaike
343 information criterion (AIC) (Grace et al., 2010).

344 We used two strategies to validate our SEM models and generate statistics of the models'
345 predictive power. The first strategy was inspired by 'null-model' analyses in ecology (Gotelli & Ulrich,
346 2012), and tests the assumption that the effects of *Sphagnum* traits in predicting microbial community
347 composition and microbial traits are not random and driven by changes in *Sphagnum* traits. To test this
348 assumption, we randomized *Sphagnum* trait matrices to break any structure in the data. We iteratively
349 and randomly shuffled the *Sphagnum* trait matrices ten times before running the SEM models. The second
350 strategy focused on the size of the data set as it can strongly influence SEM modelling (Grabowski & Porto,
351 2017; Grace et al., 2010). To do so, we iteratively reduced our entire data set by 20% by randomly
352 removing one replicate from the dataset. In other words, we retained four out of five replicates before
353 running the SEM models. We repeated this step five times, until all possible combinations were covered.
354 For each SEM model we extracted the data relative to the adequacy of the model (*Fisher's C* statistic and
355 *P*-value) and AIC values (see model outputs in Fig. S7 and Tables S11, S12). The sensitivity analyses were
356 performed on the most relevant SEM models, where the benefits gained (ΔR^2) by including *Sphagnum*
357 traits into the models was more than 10%: decomposers single, decomposers interactions, phototrophs
358 single, and yield single.

359

360 **Results**

361 Throughout this section we refer to changes in sites (see Table 1 for sites' acronyms), which nevertheless
362 are confounded with *Sphagnum* species identity. Thus, we advise to check the Materials and methods
363 section and Supplementary materials (Fig S1, S2, S3) where we demonstrate that a potential confounding
364 effect of species and site was not an important issue.

365 ***Sphagnum* morphological and anatomical traits and metabolites**

366 PCoA analysis revealed that *Sphagnum* trait composition (anatomical and morphological traits and
367 metabolites) differed among the five sites (Fig. 2a). Three distinct groups emerged from the first PCoA
368 axis: a first group composed of *Sphagnum* from FI, a second group composed of EST and SE and a third
369 group with FR and PL. On the second PCoA axis, there was a gradient ranging from FI to FR/PL and then
370 SE/EST. This gradient was not related to any particular climatic and/or edaphic trend. Instead, it showed
371 a clear trend as *Sphagnum* from FI, PL and FR had higher capitulum sizes, water holding-capacity and/or
372 metabolites concentrations (Fig. S4, S5, Table S5), as compared to SE and EST. Specific *Sphagnum*
373 anatomical and morphological traits and metabolites varied between five *Sphagnum* species from three
374 phyla (Fig. 2b; Fig. S4, S5). We found that *Sphagnum* from FR and PL produced more total and water-
375 soluble phenols, total flavonoids and tannins than SE and FI (Fig. 2b). However, *Sphagnum* from SE, FI and
376 EST produced more polysaccharides, organic acids, symmetric and antisymmetric CH₂ than FR and PL. In
377 terms of anatomical and morphological traits, *Sphagnum* sampled from PL and FI possessed higher
378 capitulum diameter, height and volume than EST and FR. Water holding capacities, hyaline cell surface
379 and chlorocyste width were highest for *Sphagnum* from FI and FR. Even though *Sphagnum* from EST had
380 highest number of hyaline cells per leaf area, its surface of hyaline cells was smallest.

381 **Microbial community composition and trait composition**

382 Microbial community composition and microbial traits differed significantly among the five sites (Fig. 3;
383 Fig. S6-S9, Tables S5), and similar to the *Sphagnum* traits composition, no particular climatic and/or
384 edaphic trend was found neither in microbial community composition nor microbial traits (Fig. 3). The
385 first PCoA axis showed three distinct groups of microbial community composition with FR and SE aside
386 and a third group composed of PL, FI and EST (Fig. 3c). On the second axis, there was a clear separation
387 between SE and the four other sites. Microbial trait composition differed markedly across the five sites
388 (Fig. 3d). While no particular variation was observed on the second PCoA axis, sites were well separated
389 along the first PCoA axis (Fig. 3d). Overall biomass differed with *Sphagnum* phylogeny. Specifically, the
390 highest biomass of consumers and decomposers was observed in SE and FR (Fig. 3a, Fig. S6). Conversely,
391 PL and EST were characterized by low biomass of most microbial groups (Fig. 3a, Fig. S6). For community
392 weighted mean (CWM) microbial traits, we found that the microbial traits related to the growth yield
393 strategy were the most abundant in FI and SE, and the least abundant in EST (Fig. 3b, Fig. S7). Microbial
394 traits related to resource acquisition peaked in FI and EST, while stress tolerance traits were the most
395 abundant in SE (Fig. 3b, Fig. S8, S9). Despite such differences in microbial biomass and CWMs of traits
396 among sites, *Sphagnum* phylogenetic distances were weakly related to differences in microbial biomasses
397 ($P > 0.1$ in most cases) and in microbial trait composition ($P > 0.1$ in all cases; Table S4). Only the biomass
398 of flagellates ($K = 1.1$, $P = 0.03$; Table S4) was significantly related to *Sphagnum* phylogenetic distances.

399 **Predictors of microbial community and microbial traits**

400 Differences in microbial community composition and microbial traits were related to both climatic and
401 edaphic conditions and *Sphagnum* traits (Fig. 4). As *Sphagnum* trait composition was also correlated with
402 climatic and edaphic conditions (*i.e.* annual precipitation and WEOM chemistry, Fig. 4), we ran structural
403 equation models with and without *Sphagnum* anatomical and morphological traits and metabolites to

404 tease apart the effects attributable to *Sphagnum* traits and metabolites on microbial properties (Fig. 5,
405 Table S6-S10). Shifts in microbial community composition and microbial traits across *Sphagnum* species
406 were correlated with multiple climatic and edaphic variables, which together explained 27%-86% of the
407 variation of the biomass of decomposers, phototrophs and consumers, as well as of microbial trait
408 composition (Table S6). When *Sphagnum* anatomical and morphological traits and metabolites were
409 added to the SEM models, prediction accuracies for most microbial biomass and trait compositions
410 increased by 42% (Fig. 5), notably for decomposer biomass (+42%), phototrophs (+19%) and traits related
411 to growth yield (+10%). Rigorous sensitivity analyses on SEM models revealed that R^2 improvements
412 provided by the addition of *Sphagnum* traits in SEMs were robust and without bias due to possible
413 randomness in the estimations (Fig. S7, S11) or the size of the dataset (Fig. S7, Table S12). Our sensitivity
414 analyses hence indicated that microbial properties can be reasonably predicted from *Sphagnum* traits,
415 and most importantly, that such effects are complementary to environmental (*i.e.* climatic and edaphic
416 conditions) variation.

417 More precisely, most *Sphagnum* metabolites were related to microbial biomasses and/or
418 microbial trait strategies (Fig. 6). The biomass of cyanobacteria, some decomposers (*i.e.* fungi and
419 bacteria) and rotifers was positively related to water-soluble phenolic compounds, whereas microalgae
420 and testate amoebae tended to be negatively correlated to phenols (Fig. 6). *Sphagnum* anatomical and
421 morphological traits, such as the width of chlorocystes and water-holding capacity, were positively
422 correlated with the biomass of nematodes and some growth yield traits (*i.e.* respiration, biomass,
423 biovolume) and some enzymes. However, methanotrophs were negatively correlated to the same
424 *Sphagnum* traits. Most of the individual microbial traits, especially those related to growth yields
425 (microbial pigments, respiration, size), were negatively correlated to water-soluble phenols, total tannins,
426 phenols, proteins, carbohydrates and pigments while also being positively correlated to polysaccharides,

427 phenols/lignins, CH₂ compounds. Opposite trends were observed for some resource acquisition traits
428 (mostly enzymes; Fig. 6).

429

430 Discussion

431 Here we tested whether *Sphagnum* phylogeny, anatomical and morphological traits and metabolites are
432 important determinants of peatland microbial community composition and functional traits. Contrary to
433 our expectations which were based on earlier observations suggesting a high degree of similarity in
434 microbial composition among closely related *Sphagnum* species (Bragina et al., 2013b; Bragina et al.,
435 2012b; Putkinen et al., 2012), we found here that microbial community and trait composition did not vary
436 with *Sphagnum* phylogenetic distance. Our findings may indicate that certain microbial taxa and traits are
437 strongly related with particular *Sphagnum* anatomical and morphological traits and metabolites, while
438 other microbial taxa and traits are more generalist and mostly influenced by environmental (climatic and
439 edaphic) conditions. Hence, *Sphagnum* interspecific trait plasticity may drive microbial community
440 composition and functional diversity in addition to climatic and local condition variables. Our results,
441 however, need to be interpreted cautiously as *Sphagnum* species and sampling site co-varied in our study.
442 Moreover, our observations were undertaken at a single date, thereby ignoring potential seasonality.
443 Nevertheless, our study represents an important and necessary step in understanding which traits from
444 diverse *Sphagnum* species are key in shaping the *Sphagnum* microbiome along an environmental gradient.

445 In contrast to peatland plant species richness and functional diversity (Robroek et al., 2017), no
446 notable latitudinal trends, neither in microbial community composition nor trait composition, were
447 observed. Instead, climatic (*i.e.* the mean temperature of the wettest quarter and annual precipitation)
448 and edaphic (*i.e.* water table depth, *Sphagnum* water content, and nutrient availability) variables were
449 identified as important drivers of microbial community and traits. This corroborates previous studies
450 showing that global and local peatland conditions play deterministic roles in shaping microbial
451 communities and functioning (Elliott et al., 2015; Jassey et al., 2014; Urbanová & Bárta, 2016). However,
452 we show that *Sphagnum* traits, mostly metabolites, were as important as climatic and edaphic conditions

453 in driving microbial community composition and functioning (Fig. 4). Our analysis revealed that microbial
454 consumers, as well as growth yield and resource acquisition traits, generally decreased with frequent
455 rainfall, high *Sphagnum* water content, and low nutrient content. Phototrophs and decomposers,
456 however, showed opposite trends. In addition, *Sphagnum* traits were negatively correlated to
457 decomposers, but positively to growth yield and resource acquisition. While correlations between
458 microbial traits, *Sphagnum* traits and climatic and edaphic factors enabled us to assess the direction of
459 these relationships, the underlying mechanisms remain unknown, since here *Sphagnum* metabolites were
460 also driven by climatic and edaphic conditions. Using the SEM approach and taking into account the
461 response of *Sphagnum* traits to climatic and edaphic conditions, our multi-model comparisons revealed
462 that the addition of *Sphagnum* traits generally did increase the predictive power of SEMs, especially for
463 the biomass of decomposers, phototrophs, and growth yield traits, while avoiding overfitting the models.
464 This suggests that *Sphagnum* anatomical and morphological traits and metabolites are important
465 regulators of *Sphagnum*-microbial interactions.

466 Overall, *Sphagnum* anatomical and morphological traits were poor predictors of microbial
467 communities. Nevertheless, we found that the biomass of cyanobacteria, large consumers, such as
468 nematodes, and microbial traits related to growth yield (*i.e.* respiration, size and volume) and resource
469 acquisition (*i.e.* some extracellular enzymes) were positively correlated to *Sphagnum* species with high
470 capitulum size, and, hence, high water-holding capacities, and width of chlorocystes (Fig. 6). Water held
471 between leaves and hyaline cells of the capitulum provides a habitat for many microorganisms (Vitt,
472 2000), and allows them to move freely with water exchange between hyaline cells and adjacent
473 photosynthetic cells (Kostka et al., 2016). However, large *Sphagnum* species are known to maintain a more
474 stable water content under unfavorable conditions thanks to the high water-holding capacity traits of
475 their capitula (Jassey & Signarbieux, 2019). Consequently, our findings suggest that microbial communities
476 associated with *Sphagnum* species with high water-holding capacity are better protected from desiccation

477 than for those living in smaller *Sphagnum* species, while the hunting space for large consumers is less
478 limited. Indeed, habitat-size is an important factor structuring microbial communities. For example,
479 Sweeney et al (2020) found that increased root surface area improved opportunities for mycorrhizal fungi
480 colonization in grasslands. Moreover, Delgado-Baquerizo et al. (2018) highlighted habitat-size as a crucial
481 driver of soil bacterial biodiversity and functional diversity.

482 Comparative effects between *Sphagnum* anatomical and morphological traits and metabolites
483 provide evidence that *Sphagnum* metabolites play a central role in structuring microbial communities and
484 their traits. We found that the biomass of cyanobacteria, fungi, and bacteria, as well as a number of
485 resource acquisition traits, such as extracellular enzymes, were positively correlated to many metabolites,
486 including total carbohydrates, proteins, *Sphagnum* pigments, total phenols and/or tannins (Fig. 6). In
487 contrast, the biomass of microalgae and nematodes, and most of microbial growth yield traits (*i.e.*
488 microbial pigments, respiration, biomass, volume and size), were negatively correlated to *Sphagnum*
489 metabolites (Fig. 6). Our findings suggest that *Sphagnum* metabolites have diverse effects on microbial
490 communities and their traits, supporting observations that the degree of host specificity varies despite
491 *Sphagnum* phylogenetic distances (Bragina et al., 2012b). The positive links between decomposers and
492 resource acquisition traits (mostly enzyme activities), and *Sphagnum* pigments, proteins and
493 carbohydrates suggest that the activity of these microorganisms benefit *Sphagnum* growth (Kostka et al.,
494 2016). Alternatively, *Sphagnum* also releases easy-degradable carbohydrates (*i.e.* glucose) that can
495 stimulate decomposers' nutrient mineralization, which directly and positively feeds back to *Sphagnum*
496 growth, the 'host'. However, such beneficial interactions between microbes and plants often involve
497 specific metabolites (Hiruma, 2019). Our findings indeed suggest that *Sphagnum* use an array of specific
498 metabolites to regulate microbial communities and their functions. Polyphenols (*e.g.* *Sphagnum* acids)
499 are released by *Sphagnum* to interact with *Sphagnum* associated microbial communities (Hamard et al.,
500 2019; van Breemen, 1995; Verhoeven & Liefveld, 1997). Polyphenols can be associated with *Sphagnum*

501 cell walls and prohibit microbial breakdown of *Sphagnum* litter (Freeman et al., 2001; van Breemen, 1995;
502 Verhoeven & Liefveld, 1997; Verhoeven & Toth, 1995) or can be released into the environment to deter
503 or kill microorganisms (Fudyma et al., 2019; Hamard et al., 2019; Mellegård et al., 2009; Opelt et al.,
504 2007b). This likely explains the negative link between phenols and most of the microbial growth traits.
505 Cell-wall carbohydrates (e.g. sphagnum) are released slowly into the environment and thus inhibit
506 microbial activity (Stalheim et al., 2009; van Breemen, 1995) either directly by inactivation of extracellular
507 enzymes or indirectly by limiting C and N mineralization and thus microbial growth (Balance et al., 2007;
508 Hájek et al., 2011). However, additional chemical analyses as well as targeted experiments are required
509 to justify this assumption for such *Sphagnum*-microbial interactions.

510 Our findings demonstrate how soil microbial communities can be structured by *Sphagnum*
511 metabolites. Also, our findings highlight the need for more targeted *Sphagnum* metabolomic analyses to
512 identify the specific compounds involved in *Sphagnum*-microbial relationships (Chiapusio et al., 2018;
513 Fudyma et al., 2019). *Sphagnum* leachates are composed of thousands of compounds (Fudyma et al.,
514 2019; Hamard et al., 2019), and contain not only *Sphagnum* compounds but also microbial derivative
515 compounds (Hamard et al., 2019). We found that *Sphagnum* organic acids, symmetric and asymmetric
516 CH₂ (lipids and fatty acids) were positively related to microbial phototrophic traits such as microbial
517 photosynthetic pigments, photosynthesis efficiency, and C fixation. Microbial phototrophs are highly
518 diverse and abundant in *Sphagnum* mosses (Jassey et al., 2015), and are an important source of lipids
519 (Griffiths & Harrison, 2009). Hence, these findings suggest that free lipids biomarkers within the
520 *Sphagnum* surface may indicate the activity of photosynthetic microbes associated with *Sphagnum*, which
521 is in line with previous findings on the occurrence of cyanobacterial lipids in peat deposits (Huang et al.,
522 2012). In addition, phototrophic lipids also possess antimicrobial properties (Leflaive & Ten-Hage, 2007),
523 which could explain the negative relationships between lipids and microbial enzyme activities. Further
524 studies are clearly needed to assess how well molecular-derived *Sphagnum* and microbial metabolites can

525 determine microbial community and trait assemblages. In particular, more attention should be given to
526 how to extract and quantify *Sphagnum* metabolites to be able to distinguish the effects of strictly
527 *Sphagnum*-derived metabolites from microbial metabolites on microbial community composition and
528 functioning.

529 Our study showcases the key role of *Sphagnum* interspecific trait variations in driving microbial
530 community composition and microbial traits in addition to climatic and edaphic variables. Despite the
531 importance of these findings, some limitations have to be acknowledged and considered for further
532 experiments. Firstly, the confounding effect between dominant *Sphagnum* species and climate (sampled
533 one species per site), did not allow us to test for species identity and climatic effects separately. However,
534 our additional analyses showed that such a potential confounding effect was not an issue for *Sphagnum*
535 metabolites, and thus did not prevent us from assessing the direct and indirect effects of *Sphagnum* traits
536 and phylogeny in driving microbial community composition and microbial traits. Secondly, despite the
537 limited size of our dataset, sensitivity analyses showed that reducing sample size by 20 % did not
538 influenced our SEM model outputs, providing our findings with robustness and confidence.

539 In summary, our findings show that *Sphagnum* metabolites prevail over *Sphagnum* morphological
540 and anatomical traits as predictors of microbial community composition and functioning in peatlands.
541 They further reveal the possible pathways by which *Sphagnum* interacts with its microbiome. Despite the
542 importance of anatomical and morphological traits for determining *Sphagnum* ecophysiology (Oke et al.,
543 2020; S  stad & Flatberg, 1993; S  stad et al., 1999) and peatland functioning (Bengtsson et al., 2016; Laing
544 et al., 2014; Turetsky et al., 2008), we show that *Sphagnum* anatomical and morphological traits are poor
545 predictors of microbial processes compared to *Sphagnum* metabolites. This finding echoes previous work
546 in grasslands, where classical plant leaf and root traits leave a large fraction of variation in microbial
547 communities unexplained (Leff et al., 2018; but see Sweeney et al., 2020), suggesting a limited role for

548 classic morphological traits in explaining plant-microbial interactions. This can potentially be explained by
549 the fact that *Sphagnum* mosses grow in clumps, where they maintain uniform growth and
550 anatomical/morphological characteristics (Oke et al., 2020) whilst their metabolome can vary according
551 to surrounding conditions (Chiapusio et al., 2018). In addition, changes among *Sphagnum* anatomical and
552 morphological traits can take weeks or years to become apparent (Jassey & Signarbieux, 2019; Oke et al.,
553 2020), whereas changes in *Sphagnum* metabolite concentrations occur more quickly after an
554 environmental stimulus (Bakhtiari et al., 2020; Callis-Duehl et al., 2017; Defosse et al., 2021; Jassey et al.,
555 2011b) – a timescale that corresponds to microbial growth rates. As such, while the effects of climatic and
556 edaphic factors on *Sphagnum* health can be missed in anatomical/morphological traits, they can be
557 detectable in the *Sphagnum* metabolome.

558 The exact mechanisms by which *Sphagnum* mosses shape their microbiome are as yet unknown,
559 but differences in the metabolite cocktails that *Sphagnum* release into their surrounding are likely to be
560 an important factor. Interestingly to mention, a recent study found that repeated litter inputs resulted in
561 directional shifts in the composition of the soil microbiome, especially fungal communities (Veen et al.,
562 2021). The addition of grass litter to tree soils resulted in the convergence of fungal communities to those
563 found in grass soils incubated with grass litter and vice versa. Such steering effects are more likely driven
564 by different chemical composition of plant litter, suggesting that microbial communities can be selected
565 by adding particular litter, and therefore particular plant metabolite cocktails (van Dam & Bouwmeester,
566 2016; Veen et al., 2021). These results support our findings and highlight the urgent need in new
567 experiments to test whether plants select particular soil microbiome. The use of deeper plant
568 metabolomic analyses would certainly shine more light into the 'black box' of plant-microbial interactions.

569

570 **Acknowledgments**

571 This work was supported by the MIXOPEAT project (Grant No. ANR-17-CE01-0007 to VEJJ) funded by the
572 French National Research Agency. We thank the *Plateforme Analyses Physico-Chimiques* from the
573 Laboratoire Ecologie Fonctionnelle et Environnement (Toulouse) for their analyses (water extractable
574 organic matter) and for the provision of an HPLC (pigments quantification). ML was supported by the
575 National Science Foundation, Poland under grant no. UMO-2017/27/B/ST10/02228, within the framework
576 of the project ‘Carbon dioxide uptake potential of *Sphagnum* peatlands in the context of atmospheric
577 optical parameters and climate changes’ (KUSCO2). BJMR was supported by the British Ecological Society
578 research grant (SR17\1427), the Stiftelsen Anna och Gunnar Vidfelts for biologisk forskning (2018-024-
579 Vidfelts fond) and the Dutch Foundation for the Conservation of Irish bogs. Tallinn University Research
580 Fund and the project “Life Peat Restore” supported MK. We also thank Bruno Leroux from the *Fédération*
581 *Aude Claire* and the *Syndicat Forestier de Counozouls* for providing the access to the site of Counozouls.

582 **Author contribution**

583 VEJJ conceived the ideas and designed methodology with the help of AS and RC. VEJJ chose the sites with
584 the help of BJMR, ML, MK, EST and ED. VEJJ and SH collected samples with the help of MK. AS, SH and
585 VEJJ proceeded to laboratory work with the help of BP. AS analysed the data with the help of VEJJ, JMB
586 and BJMR. AS and VEJJ led the writing of the manuscript with the help of RC, JMB and BJMR. All authors
587 contributed to the drafts and gave final approval for publication.

588 **Data availability**

589 All data needed to evaluate the conclusions in the paper are present in the paper and/or the
590 Supplementary Materials. Additional data and R codes related to this paper will be publicly available
591 from Figshare (10.6084/m9.figshare.c.5191493).

592 **References**

- 593 Averill, C., Bhatnagar, J. M., Dietze, M. C., Pearse, W. D., & Kivlin, S. N. (2019). Global imprint of mycorrhizal
594 fungi on whole-plant nutrient economics. *Proceedings of the National Academy of Sciences of the*
595 *United States of America*, *116*(46), 23163–23168. doi: 10.1073/pnas.1906655116
- 596 Bakhtiari, M., Glauser, G., Defosse, E., & Rasmann, S. (2020). Ecological convergence of secondary
597 phytochemicals along elevational gradients. *New Phytologist*, *229*(3), 1755–1767. doi:
598 10.1111/nph.16966
- 599 Ballance, S., Børshheim, K. Y., Inngjerd, K., Paulsen, B. S., & Christensen, B. E. (2007). A re-examination
600 and partial characterisation of polysaccharides released by mild acid hydrolysis from the chlorite-
601 treated leaves of *Sphagnum papillosum*. *Carbohydrate Polymers*, *67*(1), 104–115. doi:
602 10.1016/j.carbpol.2006.04.020
- 603 Barberán, A., McGuire, K. L., Wolf, J. A., Jones, F. A., Wright, S. J., Turner, B. L., ... Fierer, N. (2015). Relating
604 belowground microbial composition to the taxonomic, phylogenetic, and functional trait
605 distributions of trees in a tropical forest. *Ecology Letters*, *18*(12), 1397–1405. doi: 10.1111/ele.12536
- 606 Bardgett, R. D., & Wardle, D. A. (2010). Aboveground-Belowground linkages. In *Oxford Series in Ecology*
607 *and Evolution*.
- 608 Bengtsson, F., Granath, G., & Rydin, H. (2016). Photosynthesis, growth, and decay traits in *Sphagnum* - a
609 multispecies comparison. *Ecology and Evolution*, *6*(10), 3325–3341. doi: 10.1002/ece3.2119
- 610 Bengtsson, F., Rydin, H., & Hájek, T. (2018). Biochemical determinants of litter quality in 15 species of
611 *Sphagnum*. *Plant and Soil*, *425*(1–2), 161–176. doi: 10.1007/s11104-018-3579-8
- 612 Borowik, A., & Wyszowska, J. (2016). Soil moisture as a factor affecting the microbiological and
613 biochemical activity of soil. *Plant, Soil and Environment*, *62*(6), 250–255. doi: 10.17221/158/2016-
614 PSE
- 615 Bragina, A., Berg, C., Cardinale, M., Shcherbakov, A., Chebotar, V., & Berg, G. (2012). *Sphagnum* mosses
616 harbour highly specific bacterial diversity during their whole lifecycle. *ISME Journal*, *6*(4), 802–813.
617 doi: 10.1038/ismej.2011.151
- 618 Bragina, A., Berg, C., Müller, H., Moser, D., & Berg, G. (2013). Insights into functional bacterial diversity
619 and its effects on Alpine bog ecosystem functioning. *Scientific Reports*, *3*, 1–8. doi:
620 10.1038/srep01955
- 621 Bragina, A., Cardinale, M., Berg, C., & Berg, G. (2013). Vertical transmission explains the specific
622 Burkholderia pattern in *Sphagnum* mosses at multi-geographic scale. *Frontiers in Microbiology*,
623 *4*(DEC), 1–10. doi: 10.3389/fmicb.2013.00394

624 Bragina, A., Maier, S., Berg, C., Müller, H., Chobot, V., Hadacek, F., & Berg, G. (2012). Similar diversity of
625 Alphaproteobacteria and nitrogenase gene amplicons on two related Sphagnum mosses. *Frontiers*
626 *in Microbiology*, 2(JAN), 1–10. doi: 10.3389/fmicb.2011.00275

627 Burnham, K. P., & Anderson, D. R. (2004). Multimodel inference: Understanding AIC and BIC in model
628 selection. *Sociological Methods and Research*, 33(2), 261–304. doi: 10.1177/0049124104268644

629 Burns, J. H., Anacker, B. L., Strauss, S. Y., & Burke, D. J. (2015). Soil microbial community variation
630 correlates most strongly with plant species identity, followed by soil chemistry, spatial location and
631 plant genus. *AoB PLANTS*, 7(1), 1–10. doi: 10.1093/aobpla/plv030

632 Buttler, A., Robroek, B. J. M., Laggoun-Défarge, F., Jassey, V. E. J., Pochelon, C., Bernard, G., ... Bragazza, L.
633 (2015). Experimental warming interacts with soil moisture to discriminate plant responses in an
634 ombrotrophic peatland. *Journal of Vegetation Science*, 26(5), 964–974. doi: 10.1111/jvs.12296

635 Callis-Duehl, K., Vittoz, P., Defosse, E., & Rasmann, S. (2017). Community-level relaxation of plant
636 defenses against herbivores at high elevation. *Plant Ecology*, 218(3), 291–304. doi: 10.1007/s11258-
637 016-0688-4

638 Chiapusio, G., Jassey, V. E. J., Bellvert, F., Comte, G., Weston, L. A., Delarue, F., ... Binet, P. (2018).
639 Sphagnum Species Modulate their Phenolic Profiles and Mycorrhizal Colonization of Surrounding
640 *Andromeda polifolia* along Peatland Microhabitats. *Journal of Chemical Ecology*, 44(12), 1146–1157.
641 doi: 10.1007/s10886-018-1023-4

642 Chomel, M., Guittonny-Larchevêque, M., Fernandez, C., Gallet, C., DesRochers, A., Paré, D., ... Baldy, V.
643 (2016). Plant secondary metabolites: a key driver of litter decomposition and soil nutrient cycling.
644 *Journal of Ecology*, 104(6), 1527–1541. doi: 10.1111/1365-2745.12644

645 Crowther, T. W., van den Hoogen, J., Wan, J., Mayes, M. A., Keiser, A. D., Mo, L., ... Maynard, D. S. (2019).
646 The global soil community and its influence on biogeochemistry. *Science*, 365(6455), eaav0550. doi:
647 10.1126/science.aav0550

648 De Gruyter, J., Weedon, J. T., Bazot, S., Dauwe, S., Fernandez-Garberí, P.-R., Geisen, S., ... Verbruggen, E.
649 (2020). Patterns of local, intercontinental and interseasonal variation of soil bacterial and eukaryotic
650 microbial communities. *FEMS Microbiology Ecology*, 96(3). doi: 10.1093/femsec/fiaa018

651 de Vries, F. T., Manning, P., Tallowin, J. R. B., Mortimer, S. R., Pilgrim, E. S., Harrison, K. A., ... Bardgett, R.
652 D. (2012). Abiotic drivers and plant traits explain landscape-scale patterns in soil microbial
653 communities. *Ecology Letters*, 15(11), 1230–1239. doi: 10.1111/j.1461-0248.2012.01844.x

654 Defosse, E., Pitteloud, C., Descombes, P., Glauser, G., Allard, P.-M., Walker, T. W. N., ... Rasmann, S.
655 (2021). Spatial and evolutionary predictability of phytochemical diversity. *Proceedings of the*

656 *National Academy of Sciences*, 118(3), e2013344118. doi: 10.1073/pnas.2013344118

657 Delgado-Baquerizo, M., Eldridge, D. J., Hamonts, K., Reich, P. B., & Singh, B. K. (2018). Experimentally
658 testing the species-habitat size relationship on soil bacteria: A proof of concept. *Soil Biology and*
659 *Biochemistry*, 123(August 2017), 200–206. doi: 10.1016/j.soilbio.2018.05.016

660 Elliott, D. R., Caporn, S. J. M., Nwaishi, F., Nilsson, R. H., & Sen, R. (2015). Bacterial and fungal communities
661 in a degraded ombrotrophic peatland undergoing natural and managed re-vegetation. *PLoS ONE*,
662 10(5), 1–20. doi: 10.1371/journal.pone.0124726

663 Felsenstein, J. (1985). Phylogenies and the Comparative Method. *The American Naturalist*, 125(1), 1–15.
664 doi: 10.1086/284325

665 Fick, S. E., & Hijmans, R. J. (2017). WorldClim 2: new 1-km spatial resolution climate surfaces for global
666 land areas. *International Journal of Climatology*, 37(12), 4302–4315. doi: 10.1002/joc.5086

667 Freeman, C., Ostle, N., & Kang, H. (2001). An enzymic “latch” on a global carbon store: A shortage of
668 oxygen locks up carbon in peatlands by restraining a single enzymes. *Nature*, 409(6817), 149. doi:
669 10.1038/35051650

670 Fudyma, J. D., Lyon, J., AminiTabrizi, R., Gieschen, H., Chu, R. K., Hoyt, D. W., ... Tfaily, M. M. (2019).
671 Untargeted metabolomic profiling of *Sphagnum fallax* reveals novel antimicrobial metabolites. *Plant*
672 *Direct*, 3(September), 1–17. doi: 10.1002/pld3.179

673 Geisen, S. (2020). Protists as catalyzers of microbial litter breakdown and carbon cycling at different
674 temperature regimes. *The ISME Journal*, 10–13. doi: 10.1038/s41396-020-00792-y

675 Gessner, M. O., Bauchrowitz, M. A., & Escutier, M. (1991). Extraction and quantification of ergosterol as
676 a measure of fungal biomass in leaf litter. *Microbial Ecology*, 22(1), 285–291. doi:
677 10.1007/BF02540230

678 Gilbert, D., Amblard, C., Bourdier, G., & Francez, A. J. (1998). The microbial loop at the surface of a
679 peatland: Structure, function, and impact of nutrient input. *Microbial Ecology*, 35(1), 83–93. doi:
680 10.1007/s002489900062

681 Gotelli, N. J., & Ulrich, W. (2012). Statistical challenges in null model analysis. *Oikos*, 121(2), 171–180. doi:
682 10.1111/j.1600-0706.2011.20301.x

683 Grabowski, M., & Porto, A. (2017). How many more? Sample size determination in studies of
684 morphological integration and evolvability. *Methods in Ecology and Evolution*, 8(5), 592–603. doi:
685 10.1111/2041-210X.12674

686 Grace, J. B., Adler, P. B., Stanley Harpole, W., Borer, E. T., & Seabloom, E. W. (2014). Causal networks
687 clarify productivity-richness interrelations, bivariate plots do not. *Functional Ecology*, 28(4), 787–

688 798. doi: 10.1111/1365-2435.12269

689 Grace, J. B., Anderson, T. M., Olff, H., & Scheiner, S. M. (2010). On the specification of structural equation
690 models for ecological systems. *Ecological Monographs*, 80(1), 67–87. doi: 10.1890/09-0464.1

691 Gralka, M., Szabo, R., Stocker, R., & Cordero, O. X. (2020). Trophic Interactions and the Drivers of Microbial
692 Community Assembly. *Current Biology*, 30(19), R1176–R1188. doi: 10.1016/j.cub.2020.08.007

693 Griffiths, M. J., & Harrison, S. T. L. (2009). Lipid productivity as a key characteristic for choosing algal
694 species for biodiesel production. *Journal of Applied Phycology*, 21(5), 493–507. doi: 10.1007/s10811-
695 008-9392-7

696 Gui, H., Hyde, K., Xu, J., & Mortimer, P. (2017). Arbuscular mycorrhiza enhance the rate of litter
697 decomposition while inhibiting soil microbial community development. *Scientific Reports*,
698 7(February), 1–10. doi: 10.1038/srep42184

699 Hájek, T., Ballance, S., Limpens, J., Zijlstra, M., & Verhoeven, J. T. A. (2011). Cell-wall polysaccharides play
700 an important role in decay resistance of Sphagnum and actively depressed decomposition in vitro.
701 *Biogeochemistry*, 103(1), 45–57. doi: 10.1007/s10533-010-9444-3

702 Hamard, S., Robroek, B. J. M., Allard, P.-M., Signarbieux, C., Zhou, S., Saesong, T., ... Jassey, V. E. J. (2019).
703 Effects of Sphagnum Leachate on Competitive Sphagnum Microbiome Depend on Species and Time.
704 *Frontiers in Microbiology*, 10(September), 1–17. doi: 10.3389/fmicb.2019.02042

705 Hansen, A. M., Kraus, T. E. C., Pellerin, B. A., Fleck, J. A., Downing, B. D., & Bergamaschi, B. A. (2016).
706 Optical properties of dissolved organic matter (DOM): Effects of biological and photolytic
707 degradation. *Limnology and Oceanography*, 61(3), 1015–1032. doi: 10.1002/lno.10270

708 Hiruma, K. (2019). Roles of Plant-Derived Secondary Metabolites during Interactions with Pathogenic and
709 Beneficial Microbes under Conditions of Environmental Stress. *Microorganisms*, 7(9), 362. doi:
710 10.3390/microorganisms7090362

711 Hodgkins, S. B., Tfaily, M. M., McCalley, C. K., Logan, T. A., Crill, P. M., Saleska, S. R., ... Chanton, J. P. (2014).
712 Changes in peat chemistry associated with permafrost thaw increase greenhouse gas production.
713 *Proceedings of the National Academy of Sciences*, 111(16), 5819–5824. doi:
714 10.1073/pnas.1314641111

715 Hu, L., Robert, C. A. M., Cadot, S., Zhang, X., Ye, M., Li, B., ... Erb, M. (2018). Root exudate metabolites
716 drive plant-soil feedbacks on growth and defense by shaping the rhizosphere microbiota. *Nature*
717 *Communications*, 9(1), 1–13. doi: 10.1038/s41467-018-05122-7

718 Huang, X., Xue, J., Zhang, J., Qin, Y., Meyers, P. A., & Wang, H. (2012). Effect of different wetness conditions
719 on Sphagnum lipid composition in the Erxianyan peatland, central China. *Organic Geochemistry*, 44,

720 1–7. doi: 10.1016/j.orggeochem.2011.12.005

721 Isoviita, P. (1966). Studies on Sphagnum L . I . Nomenclatural revision of the European taxa. *Annales*
722 *Botanici Fennici*, 3(2), 199–264. Retrieved from <https://www.jstor.org/stable/23724595>

723 Jaffrain, J., Gérard, F., Meyer, M., & Ranger, J. (2007). Assessing the Quality of Dissolved Organic Matter
724 in Forest Soils Using Ultraviolet Absorption Spectrophotometry. *Soil Science Society of America*
725 *Journal*, 71(6), 1851–1858. doi: 10.2136/sssaj2006.0202

726 Jassey, V. E. J., Chiapusio, G., Gilbert, D., Buttler, A., Toussaint, M.-L., & Binet, P. (2011). Experimental
727 climate effect on seasonal variability of polyphenol/phenoxidase interplay along a narrow fen-bog
728 ecological gradient in Sphagnum fallax. *Global Change Biology*, 17(9), 2945–2957. doi:
729 10.1111/j.1365-2486.2011.02437.x

730 Jassey, V. E. J., Gilbert, D., Binet, P., Toussaint, M.-L., & Chiapusio, G. (2011). Effect of a temperature
731 gradient on Sphagnum fallax and its associated living microbial communities: a study under
732 controlled conditions. *Canadian Journal of Microbiology*, 57(3), 226–235. doi: 10.1139/w10-116

733 Jassey, V. E. J. J., & Signarbieux, C. (2019). Effects of climate warming on Sphagnum photosynthesis in
734 peatlands depend on peat moisture and species-specific anatomical traits . *Global Change Biology*,
735 25(May), 1–12. doi: 10.1111/gcb.14788

736 Jassey, V. E. J., Lamentowicz, L., Robroek, B. J. M., Gabka, M., Rusińska, A., & Lamentowicz, M. (2014).
737 Plant functional diversity drives niche-size-structure of dominant microbial consumers along a poor
738 to extremely rich fen gradient. *Journal of Ecology*, 102(5), 1150–1162. doi: 10.1111/1365-
739 2745.12288

740 Jassey, V. E. J., Reczuga, M. K., Zielińska, M., Słowińska, S., Robroek, B. J. M., Mariotte, P., ... Buttler, A.
741 (2018). Tipping point in plant–fungal interactions under severe drought causes abrupt rise in
742 peatland ecosystem respiration. *Global Change Biology*, 24(3), 972–986. doi: 10.1111/gcb.13928

743 Jassey, V. E. J., Signarbieux, C., Hättenschwiler, S., Bragazza, L., Buttler, A., Delarue, F., ... Robroek, B. J. M.
744 (2015). An unexpected role for mixotrophs in the response of peatland carbon cycling to climate
745 warming. *Scientific Reports*, 5, 1–10. doi: 10.1038/srep16931

746 Kostka, J. E., Weston, D. J., Glass, J. B., Lilleskov, E. A., Shaw, A. J., & Turetsky, M. R. (2016). The Sphagnum
747 microbiome: New insights from an ancient plant lineage. *New Phytologist*, 211(1), 57–64. doi:
748 10.1111/nph.13993

749 Laine, A. M., Lindholm, T., Nilsson, M., Kutznetsov, O., Jassey, V. E. J., & Tuittila, E. (2021). Functional
750 diversity and trait composition of vascular plant and Sphagnum moss communities during peatland
751 succession across land uplift regions . *Journal of Ecology*. doi: 10.1111/1365-2745.13601

752 Laing, C. G., Granath, G., Belyea, L. R., Allton, K. E., & Rydin, H. (2014). Tradeoffs and scaling of functional
753 traits in Sphagnum as drivers of carbon cycling in peatlands. *Oikos*, *123*(7), 817–828. doi:
754 10.1111/oik.01061

755 Laliberté, E., Legendre, P., & Shipley, B. (2015). FD: measuring functional diversity from multiple traits,
756 and other tools for functional ecology. *R Package*, Version 1.0-12.

757 Lefcheck, J. S. (2016). piecewiseSEM: Piecewise structural equation modelling in r for ecology, evolution,
758 and systematics. *Methods in Ecology and Evolution*, *7*(5), 573–579. doi: 10.1111/2041-210X.12512

759 Leff, J. W., Bardgett, R. D., Wilkinson, A., Jackson, B. G., Pritchard, W. J., De Long, J. R., ... Fierer, N. (2018).
760 Predicting the structure of soil communities from plant community taxonomy, phylogeny, and traits.
761 *ISME Journal*, *12*(7), 1794–1805. doi: 10.1038/s41396-018-0089-x

762 Leflaive, J., & Ten-Hage, L. (2007). Algal and cyanobacterial secondary metabolites in freshwaters: A
763 comparison of allelopathic compounds and toxins. *Freshwater Biology*, *52*(2), 199–214. doi:
764 10.1111/j.1365-2427.2006.01689.x

765 Legendre, P., & Legendre, L. (2012). *Numerical Ecology*. Elsevier Science.

766 Liang, C., Amelung, W., Lehmann, J., & Kästner, M. (2019). Quantitative assessment of microbial
767 necromass contribution to soil organic matter. *Global Change Biology*, *25*(11), 3578–3590. doi:
768 10.1111/gcb.14781

769 Liang, C., Schimel, J. P., & Jastrow, J. D. (2017). The importance of anabolism in microbial control over soil
770 carbon storage. *Nature Microbiology*, *2*(8), 1–6. doi: 10.1038/nmicrobiol.2017.105

771 Lindo, Z., & Gonzalez, A. (2010). The bryosphere: An integral and influential component of the Earth's
772 biosphere. *Ecosystems*, *13*(4), 612–627. doi: 10.1007/s10021-010-9336-3

773 Malik, A. A., Martiny, J. B. H., Brodie, E. L., Martiny, A. C., Treseder, K. K., & Allison, S. D. (2020). Defining
774 trait-based microbial strategies with consequences for soil carbon cycling under climate change.
775 *ISME Journal*, *14*(1), 1–9. doi: 10.1038/s41396-019-0510-0

776 Mariotte, P., Robroek, B. J. M., Jassey, V. E. J., & Buttler, A. (2015). Subordinate plants mitigate drought
777 effects on soil ecosystem processes by stimulating fungi. *Functional Ecology*, *29*(12), 1578–1586. doi:
778 10.1111/1365-2435.12467

779 Mellegård, H., Stalheim, T., Hormazabal, V., Granum, P. E., & Hardy, S. P. (2009). Antibacterial activity of
780 sphagnum acid and other phenolic compounds found in *Sphagnum papillosum* against food-borne
781 bacteria. *Letters in Applied Microbiology*, *49*(1), 85–90. doi: 10.1111/j.1472-765X.2009.02622.x

782 Mitchell, E. A. D., Gilbert, D., Buttler, A., Amblard, C., Grosvernier, P., & Gobat, J.-M. (2003). Structure of
783 microbial communities in Sphagnum peatlands and effect of atmospheric carbon dioxide

784 enrichment. *Microbial Ecology*, 46(2), 187–199. doi: 10.1007/BF03036882

785 Mommer, L., Cotton, T. E. A., Raaijmakers, J. M., Termorshuizen, A. J., van Ruijven, J., Hendriks, M., ...
786 Dumbrell, A. J. (2018). Lost in diversity: the interactions between soil-borne fungi, biodiversity and
787 plant productivity. *New Phytologist*, 218(2), 542–553. doi: 10.1111/nph.15036

788 Münkemüller, T., Lavergne, S., Bzeznik, B., Dray, S., Jombart, T., Schiffers, K., & Thuiller, W. (2012). How
789 to measure and test phylogenetic signal. *Methods in Ecology and Evolution*, 3(4), 743–756. doi:
790 10.1111/j.2041-210X.2012.00196.x

791 Nichols, J. E., & Peteet, D. M. (2019). Rapid expansion of northern peatlands and doubled estimate of
792 carbon storage. *Nature Geoscience*, 12(11), 917–921. doi: 10.1038/s41561-019-0454-z

793 Oke, T. A., Turetsky, M. R., Weston, D. J., & Shaw, J. A. (2020). Tradeoffs between phenotypic plasticity
794 and local adaptation influence the ecophysiology of the moss, *Sphagnum magellanicum*. *Oecologia*,
795 193(4), 867–877. doi: 10.1007/s00442-020-04735-4

796 Opelt, K., Berg, C., Schönmann, S., Eberl, L., & Berg, G. (2007). High specificity but contrasting biodiversity
797 of *Sphagnum*-associated bacterial and plant communities in bog ecosystems independent of the
798 geographical region. *ISME Journal*, 1(6), 502–516. doi: 10.1038/ismej.2007.58

799 Opelt, K., Chobot, V., Hadacek, F., Schönmann, S., Eberl, L., & Berg, G. (2007). Investigations of the
800 astructure and function of bacterial communities associated with *Sphagnum* mosses. *Environmental*
801 *Microbiology*, 9(11), 2795–2809. doi: 10.1111/j.1462-2920.2007.01391.x

802 Painter, T. J. (1991). Lindow man, tollund man and other peat-bog bodies: The preservative and
803 antimicrobial action of Sphagnan, a reactive glycuronoglycan with tanning and sequestering
804 properties. *Carbohydrate Polymers*, 15(2), 123–142. doi: 10.1016/0144-8617(91)90028-B

805 Pinheiro, J. C., & Bates, D. M. (2000). *Mixed-Effects Models in S and S-PLUS*. Springer.

806 Pinton, R., Varanini, Z., & Paolo, N. (2001). *The rhizosphere: biochemistry and organic substances at the*
807 *soil–plant interface*. New York: Marcel Dekker, Inc.

808 Putkinen, A., Larmola, T., Tuomivirta, T., Siljanen, H. M. P., Bodrossy, L., Tuittila, E. S., & Fritze, H. (2012).
809 Water dispersal of methanotrophic bacteria maintains functional methane oxidation in *Sphagnum*
810 mosses. *Frontiers in Microbiology*, 3(JAN), 1–10. doi: 10.3389/fmicb.2012.00015

811 R Core Team. (2019). *R: A language and environment for statistical computing*. Vienna, Austria: R
812 Foundation for Statistical Computing. Retrieved from <http://www.r-project.org/>

813 Rasmussen, S., Peters, G., & Rudolph, H. (1995). Regulation of phenylpropanoid metabolism by exogenous
814 precursors in axenic cultures of *Sphagnum fallax*. *Physiologia Plantarum*, 95(1), 83–90. doi:
815 10.1111/j.1399-3054.1995.tb00812.x

816 Rasmussen, S., Wolff, C., & Rudolph, H. (1995). Compartmentalization of phenolic constituents in
817 sphagnum. *Phytochemistry*, *38*(1), 35–39. doi: 10.1016/0031-9422(94)00650-I

818 Robroek, B. J. M., Jassey, V. E. J., Kox, M. A. R., Berendsen, R. L., Mills, R. T. E., Cécillon, L., ... Bodelier, P.
819 L. E. (2015). Peatland vascular plant functional types affect methane dynamics by altering microbial
820 community structure. *Journal of Ecology*, *103*(4), 925–934. doi: 10.1111/1365-2745.12413

821 Robroek, B. J. M., Jassey, V. E. J., Payne, R. J., Martí, M., Bragazza, L., Bleeker, A., ... Verhoeven, J. T. A.
822 (2017). Taxonomic and functional turnover are decoupled in European peat bogs. *Nature*
823 *Communications*, *8*(1). doi: 10.1038/s41467-017-01350-5

824 Robroek, B. J. M., Martí, M., Svensson, B. H., Dumont, M. G., Veraart, A. J., & Jassey, V. E. J. (2021).
825 Rewiring of peatland plant–microbe networks outpaces species turnover. *Oikos*, *130*(3), 339–353.
826 doi: 10.1111/oik.07635

827 Rudolph, H., & Samland, J. (1985). Occurrence and metabolism of sphagnum acid in the cell walls of
828 bryophytes. *Phytochemistry*, *24*(4), 745–749. doi: 10.1016/S0031-9422(00)84888-8

829 Rydin, H., & Jeglum, J. K. (2006). *The biology of peatlands*. United Kingdom Oxford: Oxford University
830 Press.

831 Såstad, S.M., & Flatberg, K. I. (1993). Leaf morphology of *Sphagnum strictum* in Norway, related to habitat
832 characteristics. *Lindbergia*, *18*(2), 71–77. doi: 10.2307/20149834

833 Såstad, Sigurd M., Pedersen, B., & Digre, K. (1999). Habitat-specific genetic effects on growth rate and
834 morphology across pH and water-level gradients within a population of the moss *Sphagnum*
835 *angustifolium* (Sphagnaceae). *American Journal of Botany*, *86*(12), 1687–1698. doi:
836 10.2307/2656667

837 Schellekens, J., Bindler, R., Martínez-Cortizas, A., McClymont, E. L., Abbott, G. D., Biester, H., ... Buurman,
838 P. (2015). Preferential degradation of polyphenols from *Sphagnum* – 4-Isopropenylphenol as a proxy
839 for past hydrological conditions in *Sphagnum*-dominated peat. *Geochimica et Cosmochimica Acta*,
840 *150*, 74–89. doi: <https://doi.org/10.1016/j.gca.2014.12.003>

841 Schlesinger, W. H., & Andrews, J. A. (2000). Soil respiration and the global carbon cycle. *Biogeochemistry*,
842 *48*, 7–20. doi: 10.1023/A:1006247623877

843 Singh, B. K., Bardgett, R. D., Smith, P., & Reay, D. S. (2010). Microorganisms and climate change: Terrestrial
844 feedbacks and mitigation options. *Nature Reviews Microbiology*, *8*(11), 779–790. doi:
845 10.1038/nrmicro2439

846 Singh, B. K., Dawson, L. A., Macdonald, C. A., & Buckland, S. M. (2009). Impact of biotic and abiotic
847 interaction on soil microbial communities and functions: A field study. *Applied Soil Ecology*, *41*(3),

848 239–248. doi: 10.1016/j.apsoil.2008.10.003

849 Stalheim, T., Ballance, S., Christensen, B. E., & Granum, P. E. (2009). Sphagnum - A pectin-like polymer
850 isolated from Sphagnum moss can inhibit the growth of some typical food spoilage and food
851 poisoning bacteria by lowering the pH. *Journal of Applied Microbiology*, *106*(3), 967–976. doi:
852 10.1111/j.1365-2672.2008.04057.x

853 Sweeney, C. J., de Vries, F. T., van Dongen, B. E., & Bardgett, R. D. (2020). Root traits explain rhizosphere
854 fungal community composition among temperate grassland plant species. *New Phytologist*, *53*(9),
855 nph.16976. doi: 10.1111/nph.16976

856 Sytiuk, A., Cereghino, R., Hamard, S., Delarue, F. F., Dorrepaal, E., Kuttim, M., ... Jassey, V. E. J. (2020).
857 Morphological and biochemical responses of Sphagnum mosses to environmental changes. *BioRxiv*,
858 2020.10.29.360388. doi: 10.1101/2020.10.29.360388

859 Tetemadze, N., Bakuridze, A., Jokhadze, M., & Machutadze, I. (2018). Peculiarities of the composition of
860 acids in Sphagnum species of the percolation bog of the Kolkheti lowland. *Annals of Agrarian Science*,
861 *16*(2), 222–225. doi: 10.1016/j.aasci.2018.04.012

862 Turetsky, M. R. (2003). New Frontiers in Bryology and Lichenology The Role of Bryophytes in Carbon and
863 Nitrogen Cycling. *The Bryologist*, *106*(3), 395–409. doi: 10.1016/S1364-8152(03)00155-5

864 Turetsky, M. R., Crow, S. E., Evans, R. J., Vitt, D. H., & Wieder, R. K. (2008). Trade-offs in resource allocation
865 among moss species control decomposition in boreal peatlands. *Journal of Ecology*, *96*(6), 1297–
866 1305. doi: 10.1111/j.1365-2745.2008.01438.x

867 Urbanová, Z., & Bárta, J. (2016). Effects of long-term drainage on microbial community composition vary
868 between peatland types. *Soil Biology and Biochemistry*, *92*, 16–26. doi:
869 10.1016/j.soilbio.2015.09.017

870 van Breemen, N. (1995). How Sphagnum bogs down other plants. *Trends in Ecology & Evolution*, *10*(7),
871 270–275. doi: 10.1016/0169-5347(95)90007-1

872 van Dam, N. M., & Bouwmeester, H. J. (2016). Metabolomics in the Rhizosphere: Tapping into
873 Belowground Chemical Communication. *Trends in Plant Science*, *21*(3), 256–265. doi:
874 10.1016/j.tplants.2016.01.008

875 Veen, G. F. (Ciska), ten Hooven, F. C., Weser, C., & Hannula, S. E. (2021). Steering the soil microbiome by
876 repeated litter addition. *Journal of Ecology*, *9*(1), 1365-2745.13662. doi: 10.1111/1365-2745.13662

877 Verhoeven, J. T. A., & Liefveld, W. M. (1997). The ecological significance of organochemical compounds in
878 Sphagnum. *Acta Botanica Neerlandica*, *46*(2), 117–130. doi: 10.1111/plb.1997.46.2.117

879 Verhoeven, J. T. A., & Toth, E. (1995). Decomposition of Carex and Sphagnum litter in fens: Effect of litter

880 quality and inhibition by living tissue homogenates. *Soil Biology and Biochemistry*, 27(3), 271–275.
881 doi: 10.1016/0038-0717(94)00183-2

882 Vitt, D. H. (2000). *Peatlands : ecosystems dominated by bryophytes*.

883 Wang, C., Michalet, R., Liu, Z., Jiang, X., Wang, X., Zhang, G., ... Xiao, S. (2020). Disentangling Large- and
884 Small-Scale Abiotic and Biotic Factors Shaping Soil Microbial Communities in an Alpine Cushion Plant
885 System. *Frontiers in Microbiology*, 11(May), 1–17. doi: 10.3389/fmicb.2020.00925

886 Wardle, D. A., Bardgett, R. D. R. D., Klironomos, J. N., Setälä, H., van der Putten, W. H., Wall, D. H., ... Wall,
887 D. H. (2004). Ecological linkages between aboveground and belowground biota. *Science*, 304(5677),
888 1629–1633. doi: 10.1126/science.1094875

889

890 **Tables**

891 Table 1. Site conditions and climatic data of the study sites

Site	location	Longitude	Latitude	Altitude	Mean annual temperature	Annual precipitation	pH (pore water)*	Water table depth*	Trophic state	Dominant <i>Sphagnum</i> on the site
FR	Counozouls (France)	2°14'02.4"	42°41'19.7"	1374 m	7.9 °C	1027 mm	4.90	16.5 cm	poor fen	<i>Sphagnum warnstorffii</i>
PL	Kusowo (Poland)	16°35'12.1"	53°48'47.9"	145 m	7.3 °C	656 mm	3.56	60 cm	bog	<i>Sphagnum magellanicum</i>
EST	Männikjärve (Estonia)	26°15'03.6"	58°52'26.4"	82 m	4.9 °C	623 mm	4.11	20 cm	bog	<i>Sphagnum rubellum</i>
FI	Siikaneva (Finland)	24°17'17.5"	61°50'41.6"	160 m	2.9 °C	611 mm	3.86	8 cm	poor fen	<i>Sphagnum papillosum</i>
SE	Abisko (Sweden)	19°03'58.7"	68°20'43.1"	281 m	- 0.1 °C	418 mm	3.83	10 cm	bog	<i>Sphagnum balticum</i>

*Measured in early July 2018

892

893 **Figure captions**

894 **Figure 1.** *A priori* conceptual structural equation model (SEM) depicting pathways by which climate and
895 edaphic conditions (standardized data of annual precipitation (clim1), mean temperature of the wettest
896 quarter (clim2), *Sphagnum* water content (local1), PC1 of WEOM chemistry (local2), PCoA1 of *Sphagnum*
897 anatomical and morphological traits (anatom) and metabolites (metab) can affect microbial community
898 composition (PcoA1 of tot.biom=total microbial biomass; Hellinger transformation of
899 decomp.=decomposers, consum.=consumers, phototr.=phototrophs) and traits (PCoA 1 of tot.traits=total
900 traits, yield=growth yield, res.acq.=resource acquisition, stress=stress tolerance). (A) a single model, (B)
901 an interaction model, (C) a single model with *Sphagnum* traits (D) an interaction model with *Sphagnum*
902 traits. Thin lines indicate a single path, while thicker lines indicate that any climatic/edaphic parameter
903 affected each representative of microbial community composition (or the sum of them) and/or microbial
904 trait composition (or the sum of them).

905 **Figure 2.** *Sphagnum* anatomical and morphological traits and metabolites data. A) Principal coordinates
906 analysis (PCoA) on the Gower dissimilarity matrix of *Sphagnum* anatomical and morphological traits and
907 metabolites for five dominant species collected along a gradient. Groups are colored according to
908 *Sphagnum* species sampled in sites spanning from south to north. B) *Sphagnum* phylogenetic tree and
909 normalized means of *Sphagnum* anatomical and morphological traits and metabolites. The square shape
910 represents mean values of anatomical and morphological traits, while circle shape – mean values of
911 metabolites. The size of mean is represented from the smallest (the smallest circle/square) to the highest
912 (the highest circle/square) values of anatomical and morphological traits and metabolites.

913 **Figure 3.** Microbial community composition and traits composition. Upper panels: *Sphagnum*
914 phylogenetic tree with the corresponding heatmap showing the dissimilarities in (A) the composition of
915 each trophic group components in which colors represent the standardized value calculated from

916 standardized means of microbial biomass, and (B) the microbial traits composition in which colors
917 represent the standardized value calculated from the first PCoA on the Gower dissimilarity matrix of
918 microbial trait composition. Lower panels: Principal coordinates analysis (PCoA) on the Gower dissimilarity
919 matrix of (C) the microbial community composition based on the abundance of all microbes (micro-
920 eukaryotic species cyanobacteria, fungi and non-photosynthetic bacteria) and (D) the microbial traits
921 composition. Groups are colored according to *Sphagnum* species sampled in sites spanning from south to
922 north.

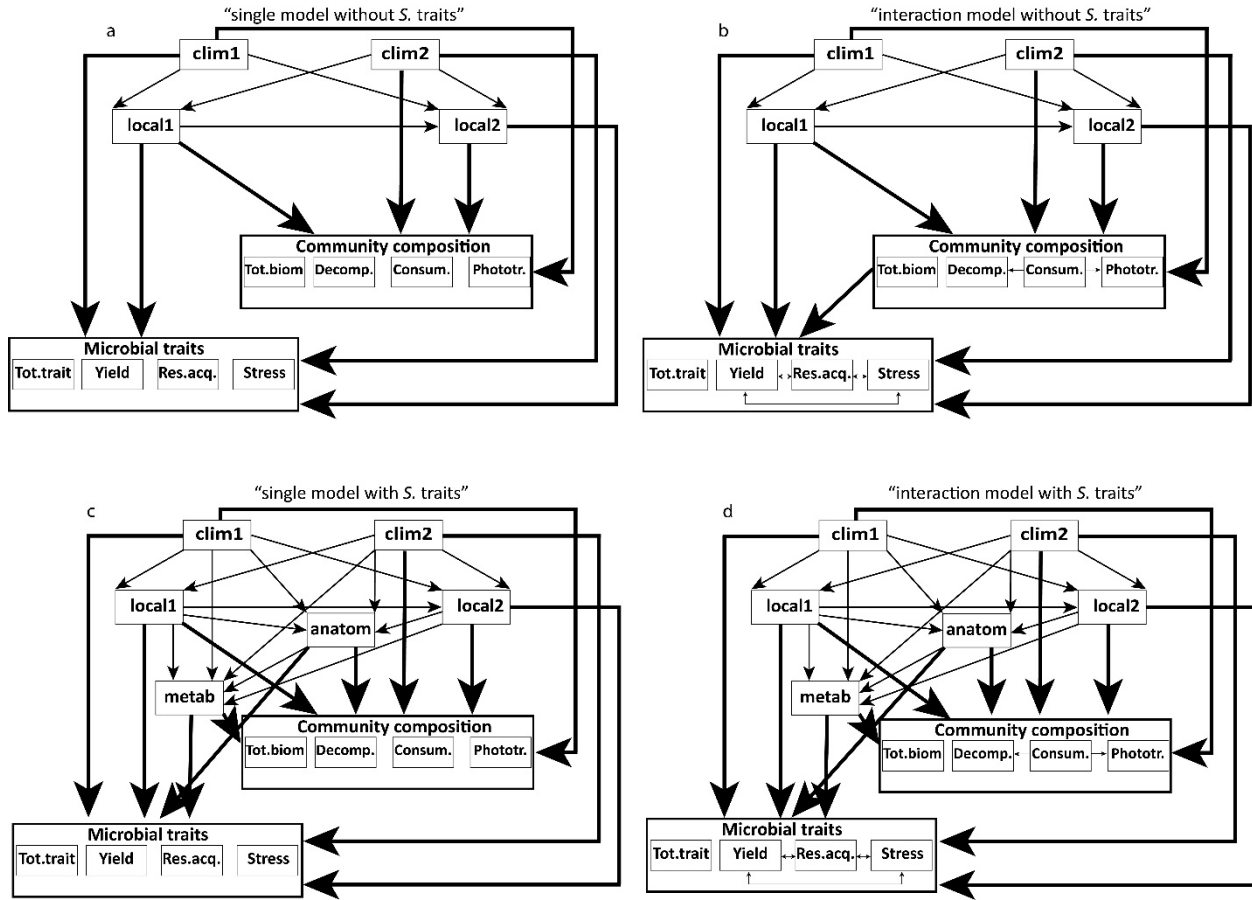
923 **Figure 4.** Correlation table on the relationships between climatic and edaphic conditions (standardized
924 data of annual precipitation (an. precip.), the mean temperature of the wettest quarter (war. temp.), PC1
925 of WEOM chemistry (WEOM. chem.), *Sphagnum* water content (*S.wat.cont.*), PCoA1 of *Sphagnum*
926 anatomical and morphological traits and metabolites (*S. traits*) and microbial community composition and
927 traits (PCoA1). Correlations with $P < 0.05$ only are shown.

928 **Figure 5.** Outputs of the SEMs when *Sphagnum* traits were included in SEMs for microbial community
929 composition and microbial traits composition: (A) the benefits gained (ΔR^2) and (B) Akaike Information
930 Criteria (AIC) values. *Full summed models= Full model with PCoA1 for total microbial biomass and PCoA1
931 for total microbial traits. All details about SEMs including R^2 , P -values, Fisher's C , path explanations are
932 provided in Tables S6-S10.

933 **Figure 6.** The relationship between differences in the microbial community composition (sum of Hellinger-
934 transformed microbial biomass per trophic group) and their traits (PCoA1 axes) and individual *Sphagnum*
935 traits. Points represent Spearman correlation coefficients (Rho) and their significance ($P < 0.05$).

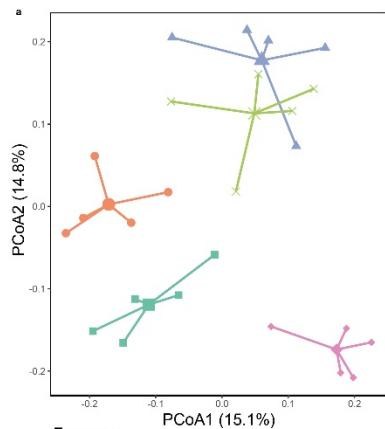
936

937 Figure 1

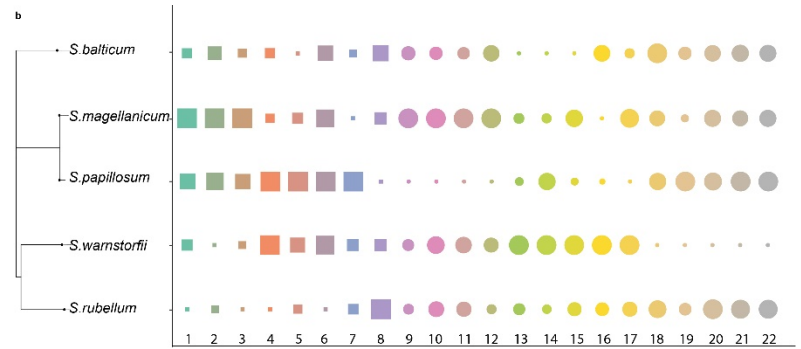


938
939

940 Figure 2



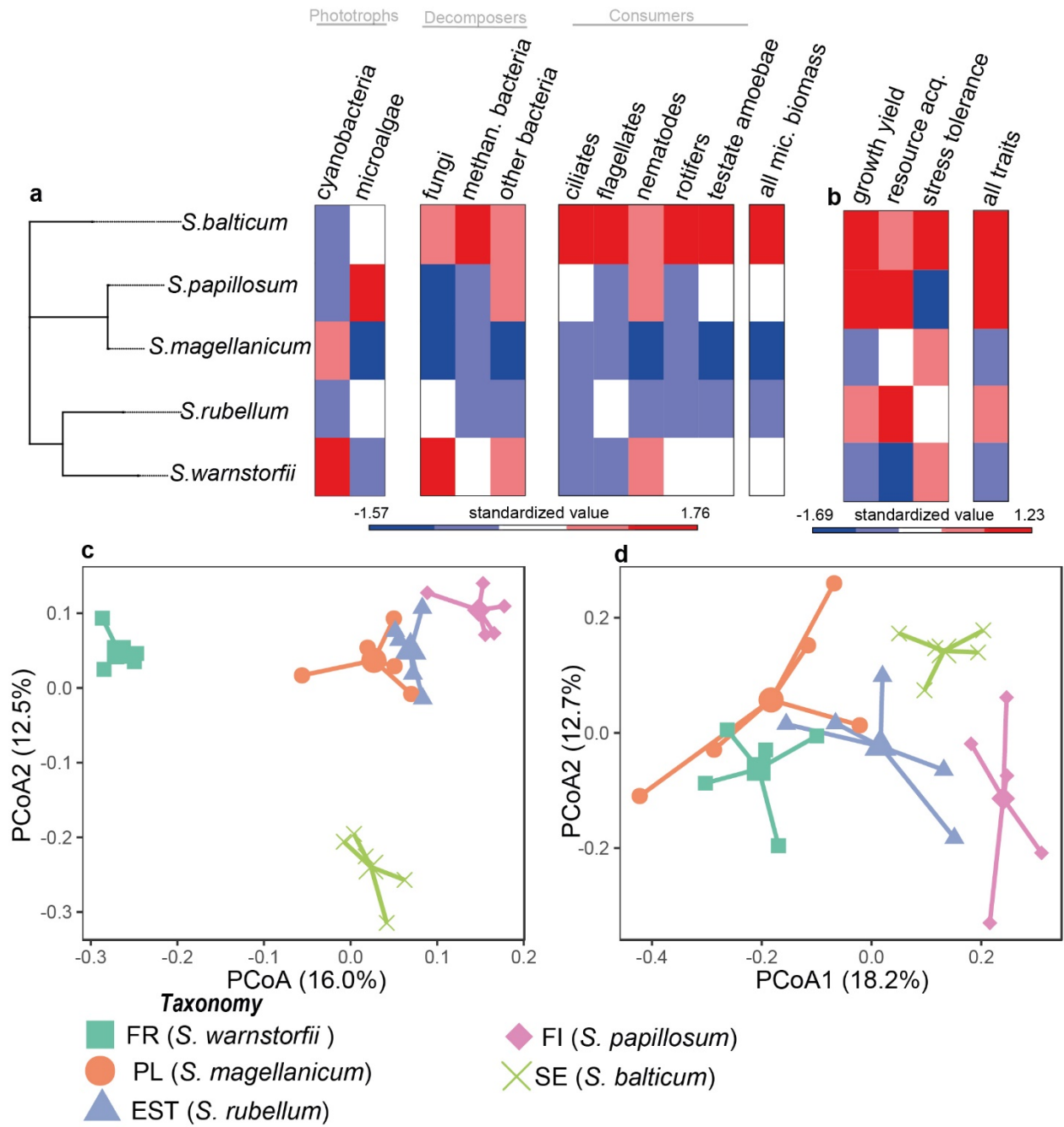
Taxonomy
 ■ FR (*S. warnstorffii*) ◆ FI (*S. papillosum*)
 ● PL (*S. magellanicum*) × SE (*S. balticum*)
 ▲ EST (*S. rubellum*)



mean

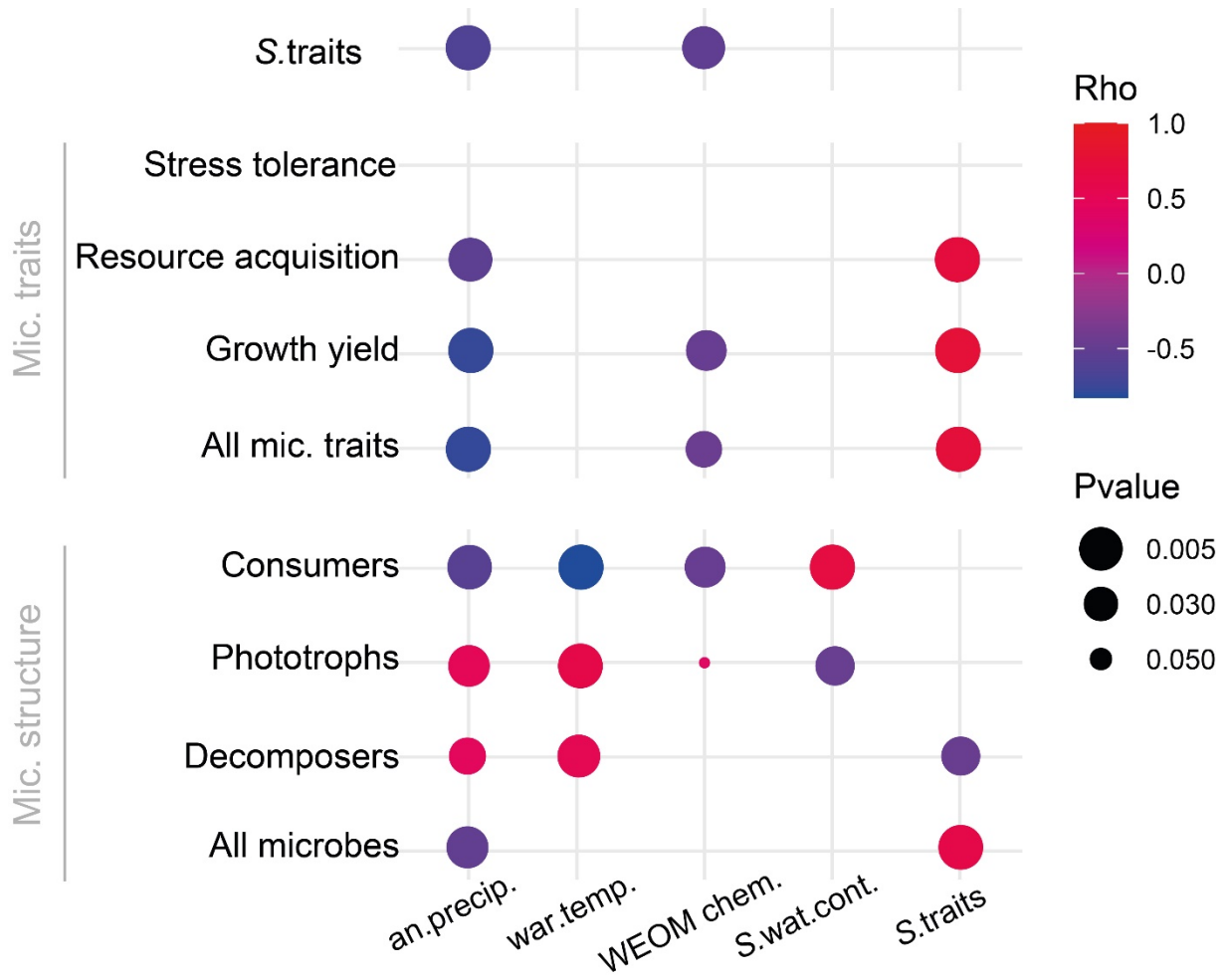
● 0.00	1 cap.diameter	6 hyaline cell surf.	9 carbohydrates	14 total flavonoids	19 phenols/lignins
● 0.25	2 cap.height	7 chlorocyste width	10 carotenoids	15 total tannins	20 organic acids
● 0.50	3 cap.volume	8 N° of hyaline cells	11 chlorophyll(a+b)	16 proline	21 symmetric CH ₂
● 0.75	4 cap.water		12 proteins	17 watersol. phenols	22 antisymmetric CH ₂
● 1.00	5 stem water		13 total phenols	18 polysaccharides	

941
942



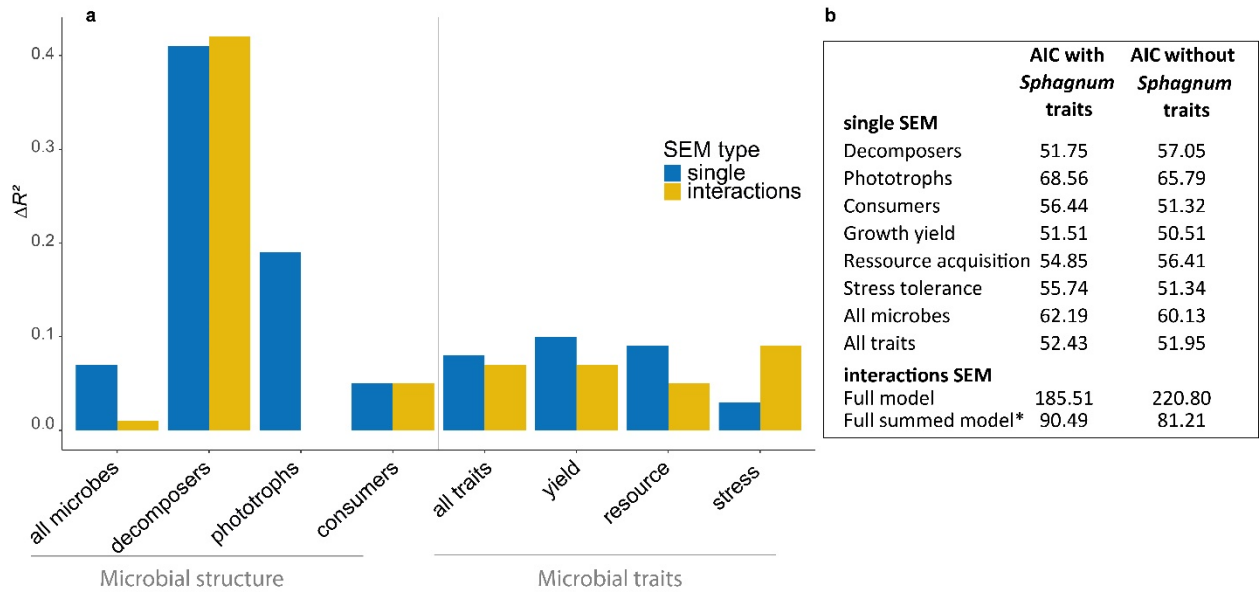
944
 945

946 Figure 4



947
948

949 Figure 5



950
951

